

The Role of H-bonds in the Solid State Organization of [1]Benzothieno[3,2-b][1]benzothiophene (BTBT) Structures : Bis(hydroxy-hexyl)-BTBT, as a Functional Derivative Offering Efficient Air Stable Organic Field Effect Transistors (OFETs).

Gilles H. Roche,^a Yu-Tang Tsai,^b Simon Clevers,^c Damien Thuau,^b Frédéric Castet,^d Yves H. Geerts,^c Joël J. E. Moreau,^a Guillaume Wantz,^{*b} and Olivier J. Dautel. ^{*a}

Table of contents

Figure S1. Synthesis of 5 according to pathway described by Hanna Jun-ichi and Kimura Hiroya	4
Figure S2. a) Molecular structure (with 50% probability displacement ellipsoids) of 1,7-diacylated BTBT (3'), showing an intramolecular interaction between a carbonyl group and a sulphur atom; b) packing as viewed down the b crystallographic direction.	7
Figure S3. a) Molecular structure of 5 (with 50% probability displacement ellipsoids), b) packing as viewed down the b axis.	8
Figure S4. a) H-bonds (Red sticks) stabilizing BTBT layers; hydrogen atoms were omitted for better clarity ; b) Two different types of H-bonds (red and orange) constituting the hydrogen bonded interlayer network. Alkyl hydrogen atoms and BTBT cores were omitted for better clarity, c) 5 smectic phase observed between cross polarizers of an optical microscope.	9
Figure S5. Major contributions to the Hirshfeld surface area for the various close intermolecular contacts in C8-BTBT-C8 and 5 (RT).	10
Figure S6. 2D fingerprint of C8-BTBT-C8 crystal structure and relative contribution for major intermolecular contacts.	11
Figure S7. 2D fingerprints of 5 crystal structure.	12
Figure S8. Superimposition of C8-BTBT-C8 (in dark) and 5 (in blue) fingerprint plots.	13
Figure S9. Superimposition of fingerprints for of C•••H (a); S•••C (b); H•••H (c) interaction in C8-BTBT-C8 (dark) and 5 (blue). (first line C8-BTBT-C8 background, second line foreground).	13
Figure S10. 2D S•••S interaction fingerprints for C8-BTBT-C8 and 5 .	14

Figure S11. Superimposition of 2D S•••S interactions fingerprints for C8-BTBT-C8 (dark) and 5 (blue).	14
Figure S12. 2,7-diacylated BTBT 3 HPLC chromatogram.	15
Figure S13. 1,7-diacylated BTBT 3' HPLC chromatogram.	15
Figure S14. Set-up used to record the FTIR behavior of 5 as a function of the temperature. 5 was disposed in a screw sealed cell built from two slices of crystalline KBr. It was deposited by drop casting between two KBr Slices. a) KBr sealed cell; b) KBr opened cell; c) KBr sealed cell disposed in the Perkin-Elmer Spectrum 100 FT-IR spectrometer.	16
Figure S15. FT-IR full spectra of a freshly recrystallized diol 5 heated from room temperature to 195°C.	17
Figure S16. a) Transfer characteristics of thermally evaporated C8-BTBT-C8 based OFET in linear regime, at VDS : -5V, b) corresponding output characteristics for different VGS. Calculated mobilities were 1.0 and 1.8 cm ² . V ⁻¹ .s ⁻¹ in linear and saturation regime respectively.	18
Figure S17. DSC thermograms of 3 (a), 3' (b) and 4 (c) realized at 10°C/min	19
Figure S18. a) 5 UV-vis spectrum in CHCl ₃ , b) Cyclic voltammogram of a 10 ⁻³ M solution of 5 in an electrolyte (0.1 M Bu ₄ NPF ₆ in tetrahydrofuran solution) at room temperature with a scan rate of 100 mV/s. Ferrocene was added to calibrate the curves. Potential are given versus E _{Fc^{+/0}} .	20
Figure S19. NMR ¹ H spectrum of 2 in CDCl ₃ .	21
Figure S20. NMR ¹ H spectrum of 2 in CDCl ₃ .	21
Figure S21. NMR ¹ H spectrum of 3 in CDCl ₃ .	22
Figure S22. NMR ¹³ C spectrum of 3 in CDCl ₃ .	22
Figure S23. NMR ¹ H spectrum of 3' in CDCl ₃ .	23
Figure S24. NMR ¹³ C spectrum of 3' in CDCl ₃ .	23
Figure S25. NMR ¹ H spectrum of 4 in CDCl ₃ .	24
Figure S26. NMR ¹³ C spectrum of 4 in CDCl ₃ .	24
Figure S27. NMR ¹ H spectrum of 5 in CDCl ₃ .	25
Figure S28. NMR ¹³ C spectrum of 5 in CDCl ₃ .	25

Experimental Details:

General: All chemicals and solvents are of reagent grade. Dichloromethane (DCM), N,N-dimethylformamide, (DMF), were dried under 4Å molecular sieves and acetic acid on 3Å molecular sieves. Melting point taken on M-560 from Buchi is uncorrected. Nuclear magnetic resonance spectra (NMR) were recorded on a Bruker 400 MHz in deuterated chloroform. MS spectra were obtained on a Synapt G2-S from Waters with a quadrupole cell collision. HPLC were performed on a column Luna 5µm NH₂ from Phenomenex at 1 mL/min with the following gradient 10%-1 min, 10% to 30%-10 min, 30%-2 min DCM/Cyclohexane. Cyclic voltammetry experiments were performed in a glove box under an atmosphere of nitrogen gas using a conventional three-electrode set-up (working, reference and counter electrode) on Potentiostat/Galvanostat Model 273A from EG&G Princeton Applied Research. Pt wires were used as working and counter electrodes and an Ag wire as pseudo reference electrode. The analyses were performed with an electrolyte [Bu₄N⁺][PF₆⁻] (0,1 M) DCM solution at room temperature at 100 mV/s (due to low solubility, the solution was saturated with the compound **5**). Ferrocenium/ferrocene (Fc/Fc⁺) redox couple were added as external reference ($E^{1/2} = +0.44$ V measured under identical conditions). Working IR temperature dependent were done with a Spectrum 100 FT-IR spectrometer from Perkin Elmer in a warming sealed cell with **5** deposited by drop casting between two KBr Slices. UV-vis spectra and Fluorescence spectra were performed with a Hewlett Packard 8453 and on a LS 55 Luminescence Spectrometer from Perkin Elmer respectively with a much diluted chloroform/Methanol 1/1 solution. DSC analyses were obtained on a DSC 200 F3 Maia from Netzsh and TGA analysis on a TGA Q50 from TA Instruments. Monocrystalline DRX were done on Oxford Diffraction Gemini-S from Agilent Technologies, powder DRX on X'pert Pro from Pan Analytical and film DRX on a Bruker D5000 and DRX temperature dependent on a Bruker D8 Advance diffractometer equipped with a MRI (Material Research Instruments) heating stage. OFET and characterization were tested on Si/SiO₂ devices Gen.4 chips from Fraunhofer IPMS (Dresden, Germany) with a bottom-gate and bottom-contact structure. The chips consist of a highly conductive n-doped Si wafer with a 230 nm thick thermally grown oxide. SiO₂ exhibits a capacity of 14.63 nF.cm⁻². On top of the SiO₂ layer, 30 nm thick Au were patterned to create source and drain contact electrodes in an interdigitated finger structure. Transistors have a channel length that varied between 2.5, 5, 10 and 20 µm, a channel width of 10 mm and a common gate contact located on the bottom of the chip. Initially, substrates were cleaned in ultrasonic baths of acetone, isopropanol and DI water for 5 minutes each at room temperature and treated with ozone plasma for an additional 15min. Electrical characterizations of the fabricated OFETs were performed using a Keithley 4200 Semiconductor Characterisation System in a glove box environment under nitrogen atmosphere. Thin films with a thickness of around 50 nm were thermally evaporated onto the OFET-chips at 1.10⁻⁶ mBar of pressure with a flow rate around 6Å/min at a temperature close to 115 °C for **5** and 98 °C for BTBT-C8. Microscopy pictures were obtained on a Leica DM6000M microscope equipped with a Leica DF 425 C camera and a Linkam warming cell. C8-BTBT-C8 were bought from Sigma Aldrich and used directly for the devices.

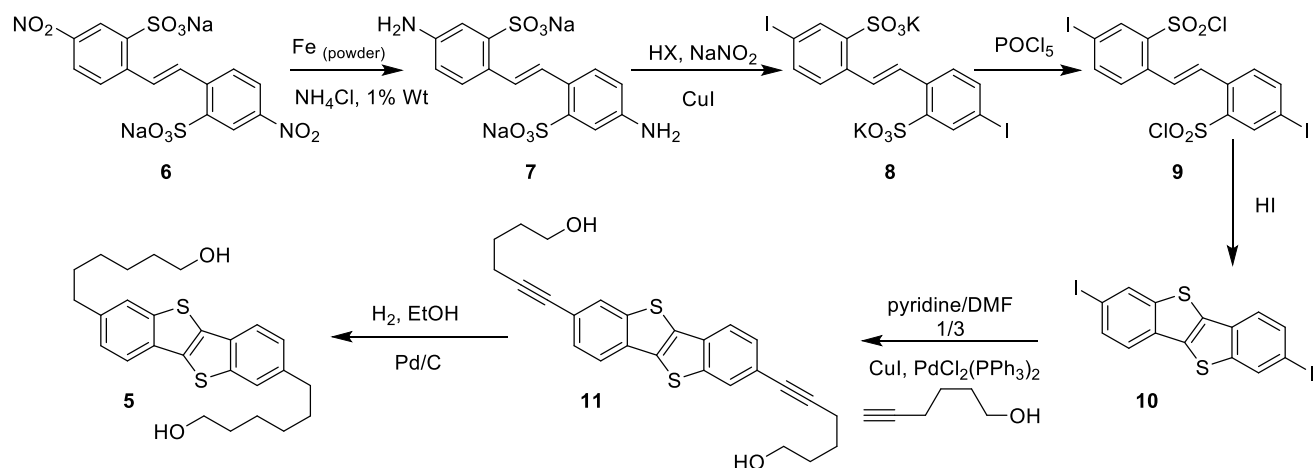
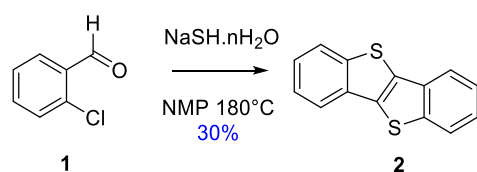


Figure S1. Synthesis of **5** according to pathway described by Hanna Jun-ichi and Kimura Hiroya.¹

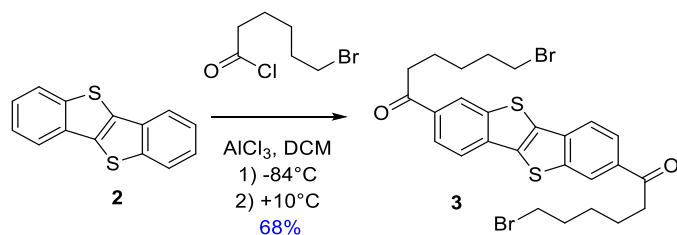
Synthetic procedures:

[1]benzothieno[3,2-*b*]-[1]benzothiophene (**2**) :



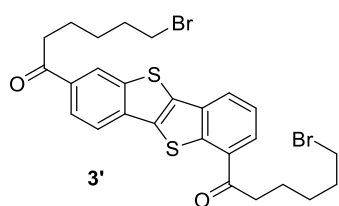
According to the procedure described by Masahiko Saito in *Tetrahedron Letters* 52 (2011) 285–288), 114 g of Sodium hydrosulfide hydrate (2 éq) were introduced in 200 mL of N-méthyl-2-pyrrolidone (NMP take a greenish color) followed by 100 g of ortho-chlorobenzaldéhyde (1 éq) (this reaction is exothermic and the reaction mixture turns red and doughy). After stirring for 1h at 80 °C, the temperature was increased to 180°C resulting in a change of the mixture color to black with blue highlights. The mixture was stirred at this temperature overnight. After cooling to room temperature, the brown mixture was poured in 1L saturated NH₄Cl solution. The red precipitate was filtered, washed twice with water and four times with acetone. The yellow precipitate obtained was dissolved in chloroform, passed on a short silica gel column and concentrated. The crude BTBT yellow flakes were further purified by recrystallization from toluene to obtain 26,0 g of orange shiny flakes of BTBT (**2**) (yield 30%). Mp: 216–217 °C (ref 1, 216–218 °C); ¹H NMR (400 MHz, CDCl₃) δ: 7.93 (ddd, J = 7.9 Hz, 1.1 Hz, 0.7 Hz, 2H), 7.89 (ddd, J = 7.9 Hz, 1.3 Hz, 0.7 Hz, 2H), 7.47 (ddd, J = 7.8 Hz, 7.2 Hz, 1.3 Hz, 2H), 7.41 (ddd, J = 8.0 Hz, 7.2 Hz, 1.4 Hz, 2H); ¹³C NMR (400 MHz, CDCl₃) δ: 121.60, 124.04, 124.88, 125.01, 133.10, 133.43, 142.25; MS (ASAP⁺) m/z(M⁺) = obsd 240.0062, calc 240.0067.

1,1'-([1]benzothieno[3,2-*b*]-[1]benzothiophene-2,7-diyl)bis(6-bromooctan-1-one) (3) :

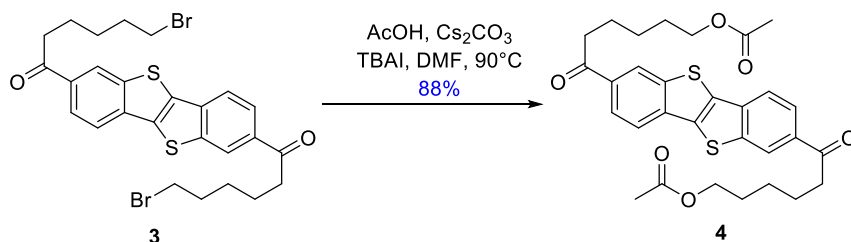


14 g of BTBT (**2**) were dissolved in 580 mL of dry DCM under argon. The solution was cooled to -10°C (a small amount of BTBT reprecipitated). 38.83 g of aluminum chloride (5 éq) were then added and the mixture took a brown color. After cooling to -84°C , 89.02 mL of 6-bromohexanoyl chloride (10 éq) were added dropwise. The mixture took yellow-red highlights. The mixture was maintained below -60°C during 2h to control the reaction to the mono-acylation and kept at $+10^\circ\text{C}$ overnight. The mixture was poured slowly on a mixture of ice and DCM. The brown color disappeared to the benefit of a yellow color. 200 ml of 1N HCl were then added and the aqueous phase was extracted 3 times with DCM. The organic layer was then washed once by a NaHCO_3 5% solution, once by saturated NaCl solution, dried over MgSO_4 and vacuum concentrated. To the crude product were added 20 g of silica gel. This solid was suspended in toluene and heated to reflux. After a hot filtration, green pale flakes crystallized on cooling. Washing the crystals twice with toluene and once with pentane, gave 20.37 g of the product (purity $>98\%$ (HPLC), yield 68%). Mp (DSC analysis): 194.1°C , $^1\text{H NMR}$ (400 MHz, CDCl_3) δ : 8.57 (d, $J = 1.0$ Hz, 2H), 8.08 (dd, $J = 8.4$ Hz, 1.5 Hz, 2H), 7.98 (d, $J = 8.4$ Hz, 2H), 3.46 (t, $J = 6.7$ Hz, 4H), 3.11 (t, $J = 7.3$ Hz, 4H), 1.96 (m, 4H), 1.84 (m, 4H), 1.60 (m, 4H) ; $^{13}\text{C NMR}$ (400 MHz, CDCl_3) δ : 199.02, 142.97, 136.45, 136.03, 134.26, 124.94, 124.70, 122.10, 38.68, 33.80, 32.76, 28.03, 23.53, 77.48, 77.16, 76.84; MS HRMS (ASAP⁺) m/z (M) = obsd 591.9748, calc 591.9741.

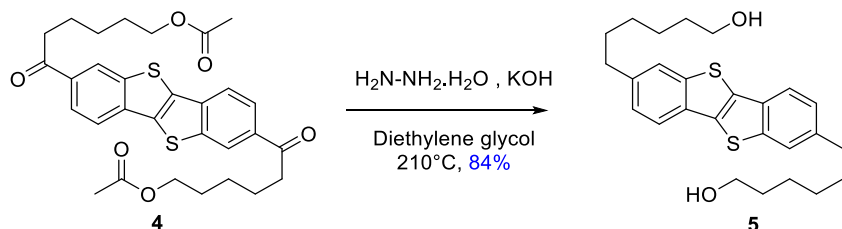
1,1'-([1]benzothieno[3,2-*b*]-[1]benzothiophene-1,7-diyl)bis(6-bromooctan-1-one) (3') :



Side product from previous reaction: Mp (DSC analysis): 157.3°C , $^1\text{H NMR}$ (400 MHz, CDCl_3) δ : 8.50 (d, $J = 1.2$ Hz, 1H), 8.11 (d, $J = 7.6$ Hz, 1H), 8.09 (d, $J = 7.6$ Hz, 1H), 8.02 (dd, $J = 8.3$ Hz, 1.2 Hz, 1H), 7.96 (d, $J = 8.4$ Hz, 1H), 7.58 (t, $J = 7.6$ Hz, 1H), 3.45 (m, 4H), 3.18 (t, $J = 7.3$ Hz, 2H), 3.07 (t, $J = 7.3$ Hz, 2H), 1.95 (m, 4H), 1.89 (m, 4H), 1.81 (m, 2H), 1.60 (m, 2H) ; $^{13}\text{C NMR}$ (400 MHz, CDCl_3) δ : 199.32, 199.06, 142.85, 142.09, 138.21, 136.60, 136.19, 134.46, 133.90, 131.30, 127.37, 126.90, 124.90, 124.54, 121.93, 38.65, 38.07, 33.72, 33.67, 32.80, 28.08, 23.63, 23.56; MS HRMS (ASAP⁺) m/z (M⁺) = obsd 592.9803, calc 592.9819.

[1]benzothieno[3,2-*b*]-[1]benzothiophene-2,7-diylbis(6-oxohexane-6,1-diyl) diacetate (4) :

23.60 g of cesium carbonate (2.1 éq) were suspended in 345 ml dry DMF under argon. 8.48 mL of dry acetic acid (4.3 éq) were introduced. A smooth heating was necessary to promote the formation of cesium carbonate. 20.5 g of compound (**3**) were added followed by 26.75 g (2 éq) of tetrabutylammonium iodide. The mixture was stirred at 90 °C for 3h. All become soluble. After cooling down to room temperature, the mixture was diluted with DCM and washed 4 times with a NaCl 8% solution and once by a saturated NaCl solution. The organic layer were dried over MgSO₄ and concentrated. The resulting solid was filtered and washed with ethyl acetate. The crude product was recrystallized in toluene and insoluble particles removed by a hot filtration. 17.65 g (yield: 88%) of greenish crystals of (**4**) were obtained. Mp (DSC analysis): 211.7 °C, ¹H NMR (400 MHz, CDCl₃) δ: 8.57 (d, J = 0.8 Hz, 2H), 8.08 (dd, J = 8.4 Hz, 1.5 Hz, 2H), 7.98 (d, J = 8.4 Hz, 2H), 4.10 (t, J = 6.7 Hz, 4H), 3.10 (t, J = 7.3 Hz, 4H), 2.05 (s, 6H), 1.85 (m, 4H), 1.72 (q, 4H), 1.55 (m, 4H) ; ¹³C NMR (400 MHz, CDCl₃) δ: 199.14, 171.39, 142.96, 136.43, 136.03, 134.29, 124.96, 124.71, 122.09, 64.49, 38.75, 28.69, 25.88, 24.08, 21.17 ; MS HRMS (ES⁺) m/z (MH⁺) = obsd 553.1719, calc 553.1719.

6,6'-([1]benzothieno[3,2-*b*]-[1]benzothiophene-2,7-diyl)bis(hexan-1-ol) (5) :

According to the Wolf-Kishner procedure described by Hideaki Ebata,⁶ 17,5 g of the diester (**4**) were introduced in 730 mL of diethylene glycol, followed by 9.97 g of KOH (5,5 éq) and 38.59 mL of ninhydrin hydrate (25 éq). The mixture was warmed to 100 °C during 1 h and the saponification of the esters resulted in a solubilization of all the material. The temperature was subsequently increased to 210 °C during 6h. The mixture was slowly cooled overnight to furnish crystals. The crystals were recovered by centrifugation and washed with water and with methanol (twice). To the crude crystals, was added 20 g of silica gel. This solid was suspended in toluene and heated to reflux. After a hot filtration, white flakes crystallized on cooling. Washing the crystals twice with toluene and once with pentane, gave 11.76 g (84%) of (**5**). Mp (DSC analysis): 186.7 °C, ¹H NMR (400 MHz, CDCl₃) δ: 7.76 (d, J = 8.1 Hz, 2H), 7.70 (s, 2H), 7.27 (d, J = 8.2 Hz, 2H), 3.65 (td, J = 6.6 Hz, J = 5.4 Hz, 4H), 2.77 (t, J = 7.4 Hz, 4H), 1.72 (m, 4H), 1.57 (m, 4H), 1.42 (m, 8H), 1.21 (t, J = 5.4 Hz, 2H) ; ¹³C NMR (400 MHz, CDCl₃) δ: 142.43, 139.85, 132.57, 131.23, 36.02, 63.01, 125.81, 123.33, 121.12, 32.71, 31.63, 29.04, 25.63; MS HRMS (ES⁺) m/z (MH⁺) = obsd 441.1924, calc 441.1922.

Crystal data for 1,7-dicylated BTBT (3'): Single crystals suitable for structural analysis were obtained by recrystallization from toluene. The X-ray measurements were carried out on crystals mounted in a cryo-loop with some paratone-N oil using a Rigaku-Oxford Diffraction Gemini diffractometer with graphite-monochromated Cu $K\alpha$ radiation ($\lambda = 1.54180 \text{ \AA}$) at 175 K. A « multi-scan » numerical absorption correction was applied. The structure was solved by iterative (charge-flipping) methods (SUPERFLIP) and refined by full-matrix non-linear least squares (CRYSTALS. The hydrogen atoms were included at idealized positions ($d(\text{C-H}) = 0.97 \text{ \AA}$ in sp^3 methylenic hydrogen atoms and $d(\text{C-H}) = 0.93 \text{ \AA}$ in $\text{sp}^2 = \text{CH}$ aromatic hydrogen atoms) and treated as riding on their parent atoms.

$\text{C}_{26}\text{H}_{26}\text{Br}_2\text{O}_2\text{S}_2$, $M = 594.41$, Colorless prism, $0.20 \times 0.25 \times 0.30 \text{ mm}^3$, *Monoclinic*, space group, $P2_1/c$, $a = 19.0077(7)$, $b = 15.6418(6)$, $c = 8.2319(3) \text{ \AA}$, $\beta = 90.654(4)^\circ$, $V = 2425.67(9) \text{ \AA}^3$, $Z = 4$, $R = 0.1194$ for 4035 observed reflections ($I > 2\sigma(I)$) and 289 variable parameters, $R_w = 0.1133$ for all data (4386).

Full crystallographic data have been deposited in CIF format at the CCSD with the number 1475860

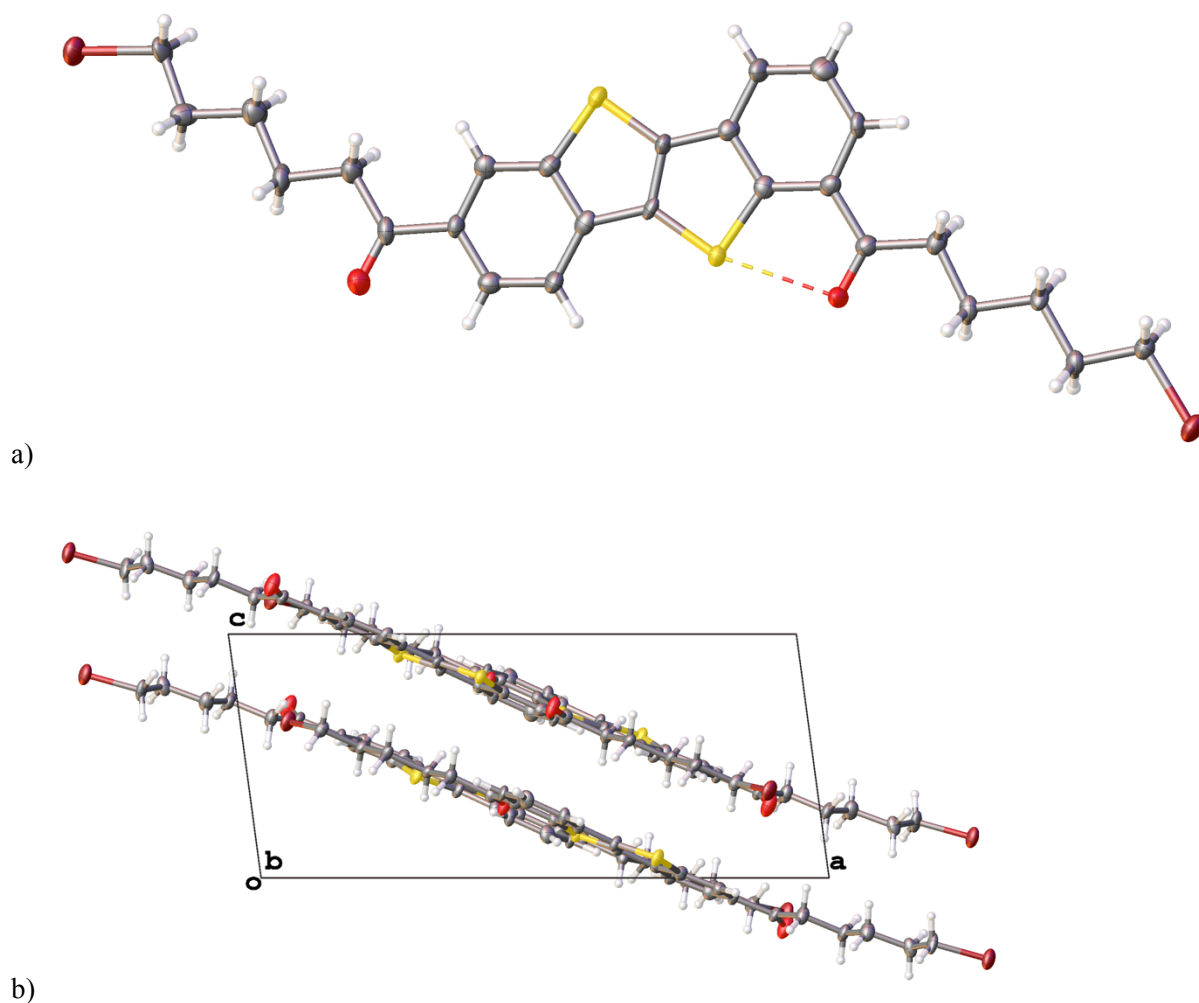


Figure S2. a) Molecular structure (with 50% probability displacement ellipsoids) of 1,7-dicylated BTBT (3'), showing an intramolecular interaction between a carbonyl group and a sulfur atom; b) packing as viewed down the b crystallographic direction.

Crystal data for (5): Single crystals suitable for structural analysis were obtained by recrystallization from chloroform. The X-ray measurements were carried out on crystals mounted in a cryo-loop with some paratone-N oil using a Rigaku-Oxford Diffraction Gemini diffractometer with graphite-monochromated Mo $K\alpha$ radiation ($\lambda = 0.71073 \text{ \AA}$) at 293 K for **5**. The structure was solved by iterative (charge-flipping) methods (SUPERFLIP) and refined by non-linear least squares (CRYSTALS). The hydrogen atoms were included at idealized positions ($d(\text{C-H}) = 0.93\text{--}0.98 \text{ \AA}$ in sp^3 methylenic hydrogen atoms, $d(\text{O-H}) = 0.82$ alcoholic hydrogen atoms, and $d(\text{C-H}) = 0.93 \text{ \AA}$ in $\text{sp}^2 = \text{CH}$ aromatic hydrogen atoms) and refined with riding constraints. Hydrogen atom of hydroxyl group are disordered over two positions.

$\text{C}_{26}\text{H}_{32}\text{O}_2\text{S}_2$, $M = 440.67$, colorless prism, $0.25 \times 0.35 \times 0.45 \text{ mm}^3$, Monoclinic, space group, $I2/a$, $a = 8.4460(3)$, $b = 5.58942(19)$, $c = 50.2534(15) \text{ \AA}$, $\beta = 92.829(3)^\circ$, $V = 2369.48(7) \text{ \AA}^3$, $Z = 4$, $R = 0.0357$ for 2345 observed reflections ($I > 2 \sigma(I)$) and 136 variable parameters, $R_w = 0.0303$ for all data (2631).

Full crystallographic data have been deposited in CIF format at the CCSD with the number 1475861

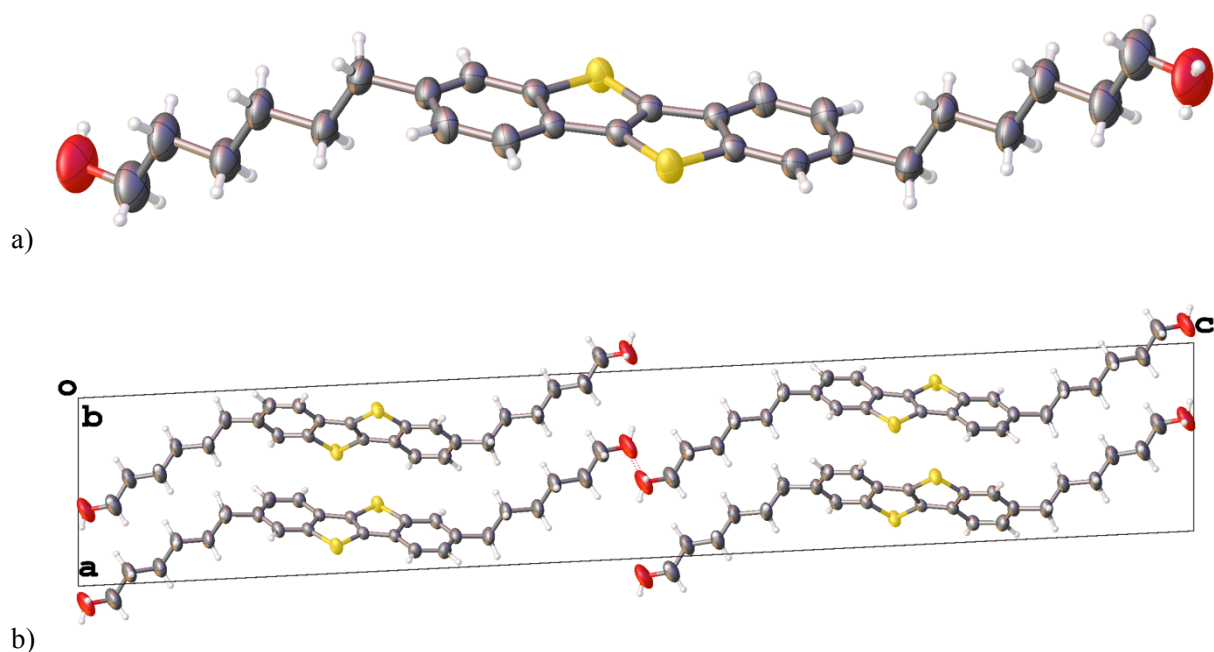


Figure S3. a) Molecular structure of **5** (with 50% probability displacement ellipsoids), b) packing as viewed down the b axis.

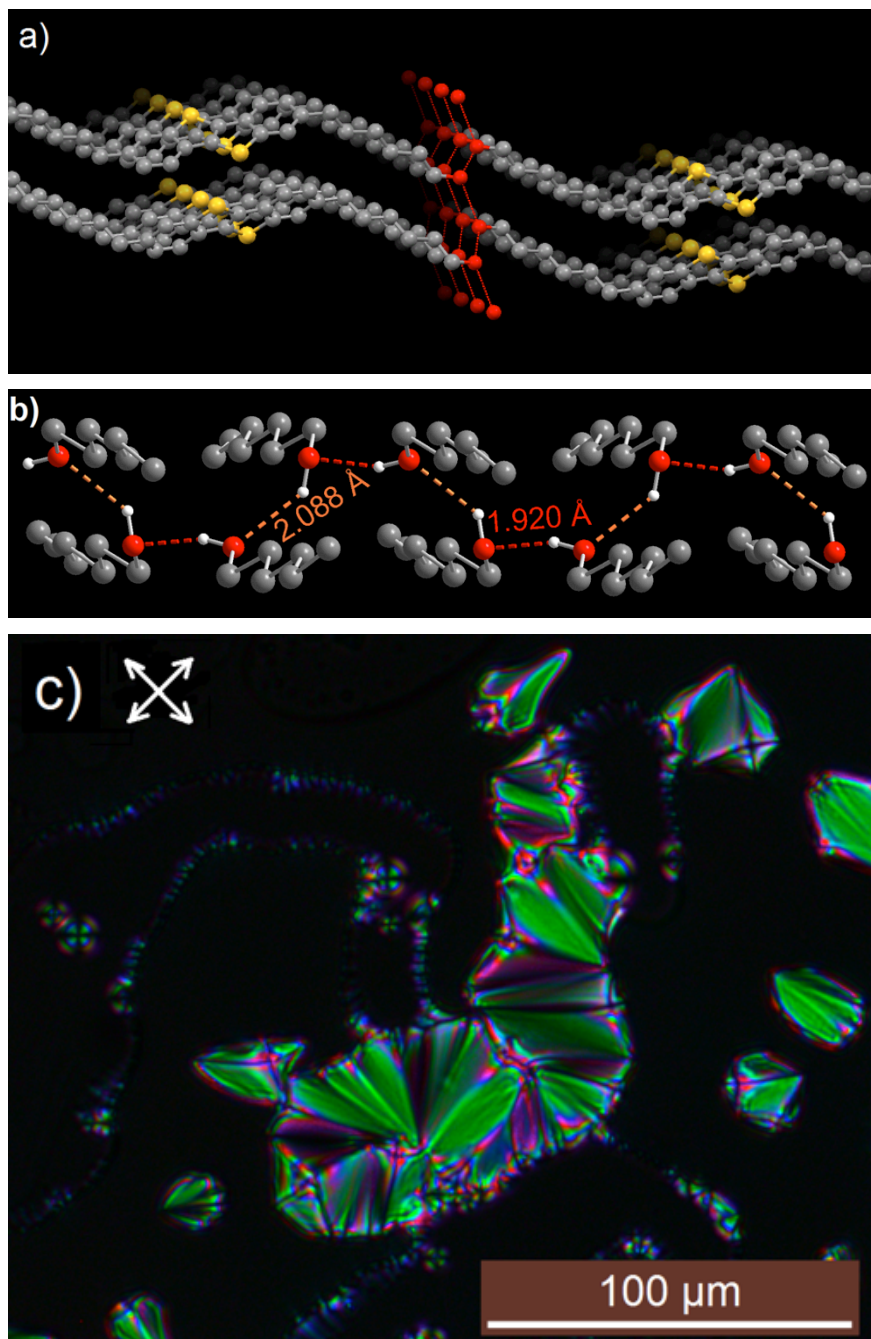


Figure S4. a) H-bonds (Red sticks) stabilizing BTBT layers; hydrogen atoms were omitted for better clarity ; b) Two different types of H-bonds (red and orange) constituting the hydrogen bonded interlayer network. Alkyl hydrogen atoms and BTBT cores were omitted for better clarity, c) **5** smectic phase observed between cross polarizers of an optical microscope.

Calculation of transfer integrals

Transfer integrals mediating the charge transfer between neighboring sites have been calculated for couples of molecules taken in their crystal geometry as the coupling terms between the many-electron wave functions of the initial and final charge-transfer states, using the semi-empirical Valence Bond / Hartree-Fock model combined with the AM1 parameterization.² These coupling terms are proportional to the weighted sum of the overlap of the orbitals belonging to the interacting molecules, the major contribution arising from the two HOMOs in the case of hole transport.

Hirshfeld Surface Analysis: Hirshfeld surfaces³ and the associated fingerprint plots⁴ were calculated using Crystal Explorer (Version 3.1), from crystal structure (file in CIF format). Bond lengths to hydrogen atoms were set to typical neutron-diffraction values (C–H = 1.083 Å). For each point on the Hirshfeld isosurface, two distances d_e , the distance from the point to the nearest nucleus external to the surface, and d_i , the distance to the nearest nucleus internal to the surface, are defined. The normalized contact distance (d_{norm}) based on d_e and d_i is given by:

$$d_{norm} = \frac{d_i - r_i^{vdW}}{r_i^{vdW}} + \frac{d_e - r_e^{vdW}}{r_e^{vdW}}$$

where r_i^{vdW} and r_e^{vdW} are the van der Waals radii of the atoms. The value d_{norm} is negative or positive depending if the intermolecular contacts are shorter or longer than the van der Waals separations. The parameter d_{norm} displays a surface with a red–white–blue color scheme, where bright red spots highlight shorter contacts, white areas represent contacts around the van der Waals separation, and blue regions are devoid of close contacts.

This type of analysis helps identify which interactions are the most dominant among neighbouring molecules. Additionally a 2D fingerprint of the molecular interactions can be represented that consists to plot d_e versus d_i . The different colors on the fingerprint plot represent the frequency of occurrence of the interaction, increasing from blue to green to red. The 2D fingerprint of the Hirshfeld surface represents a method for indicating types of intermolecular interactions and also the relative area of the surface corresponding to each kind of interaction.

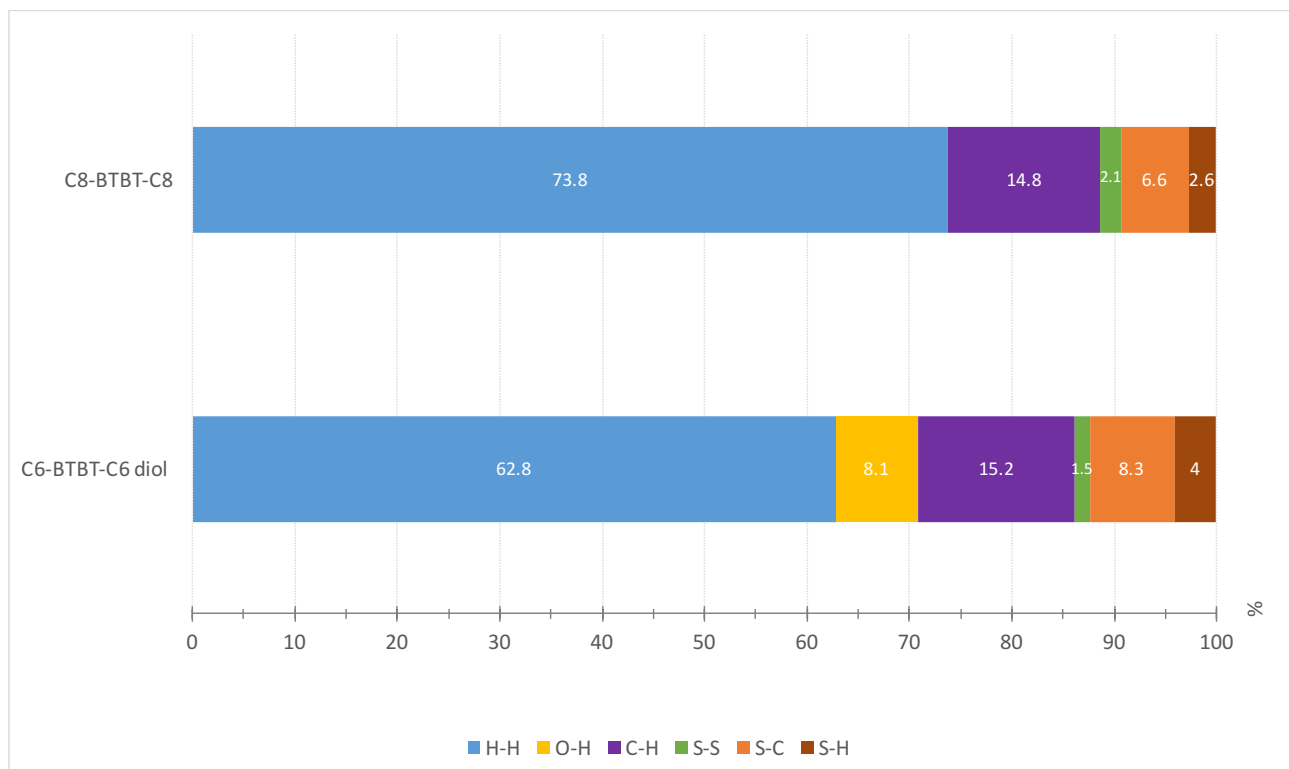


Figure S5. Major contributions to the Hirshfeld surface area for the various close intermolecular contacts in C8-BTBT-C8 and **5** (RT).

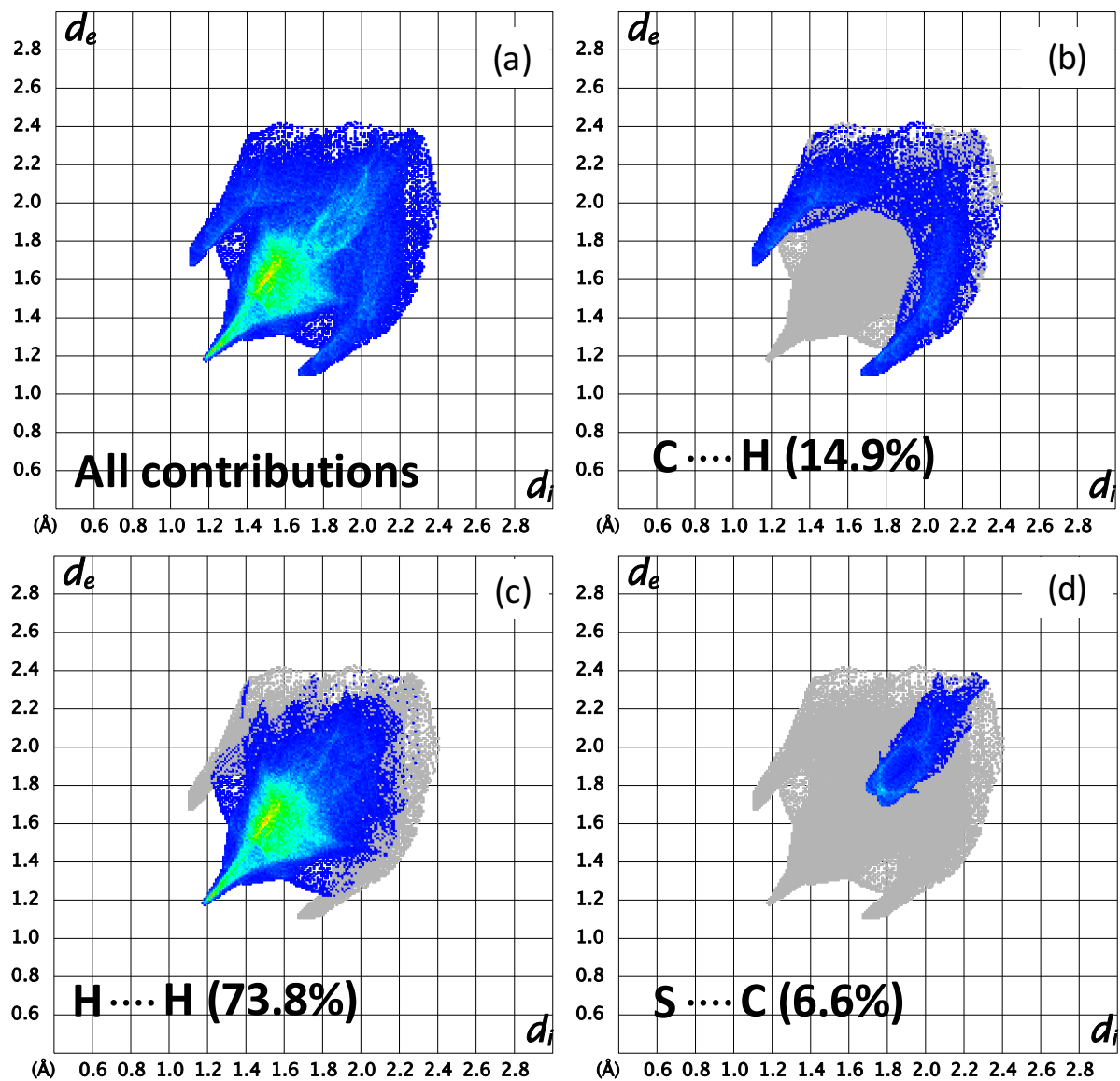


Figure S6. 2D fingerprint of C8-BTBT-C8 crystal structure and relative contribution for major intermolecular contacts.

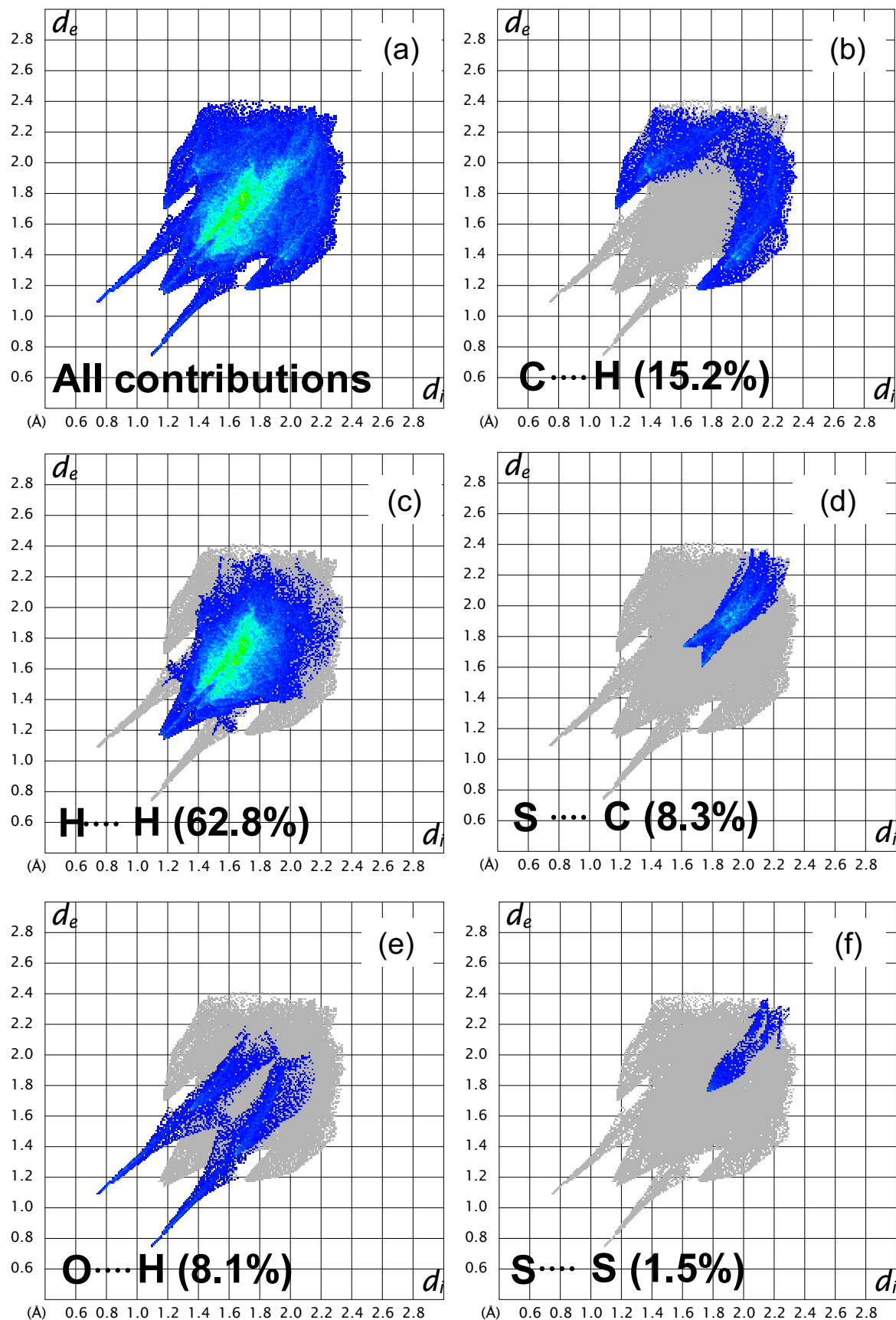


Figure S7. 2D fingerprints of 5 crystal structure.

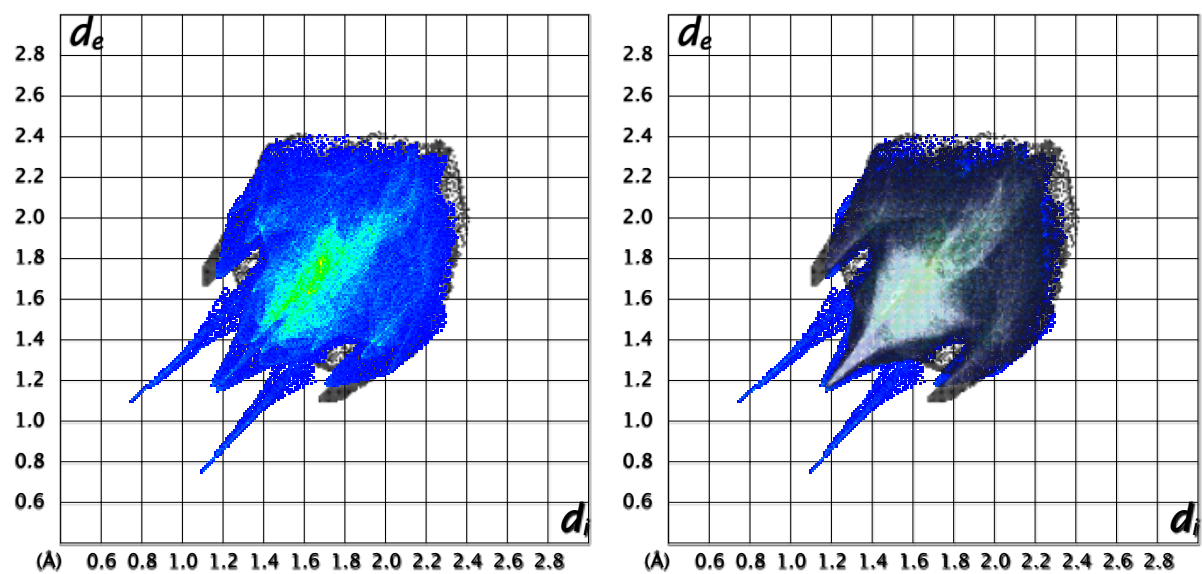


Figure S8. Superimposition of C8-BTBT-C8 (in dark) and **5** (in blue) fingerprint plots.

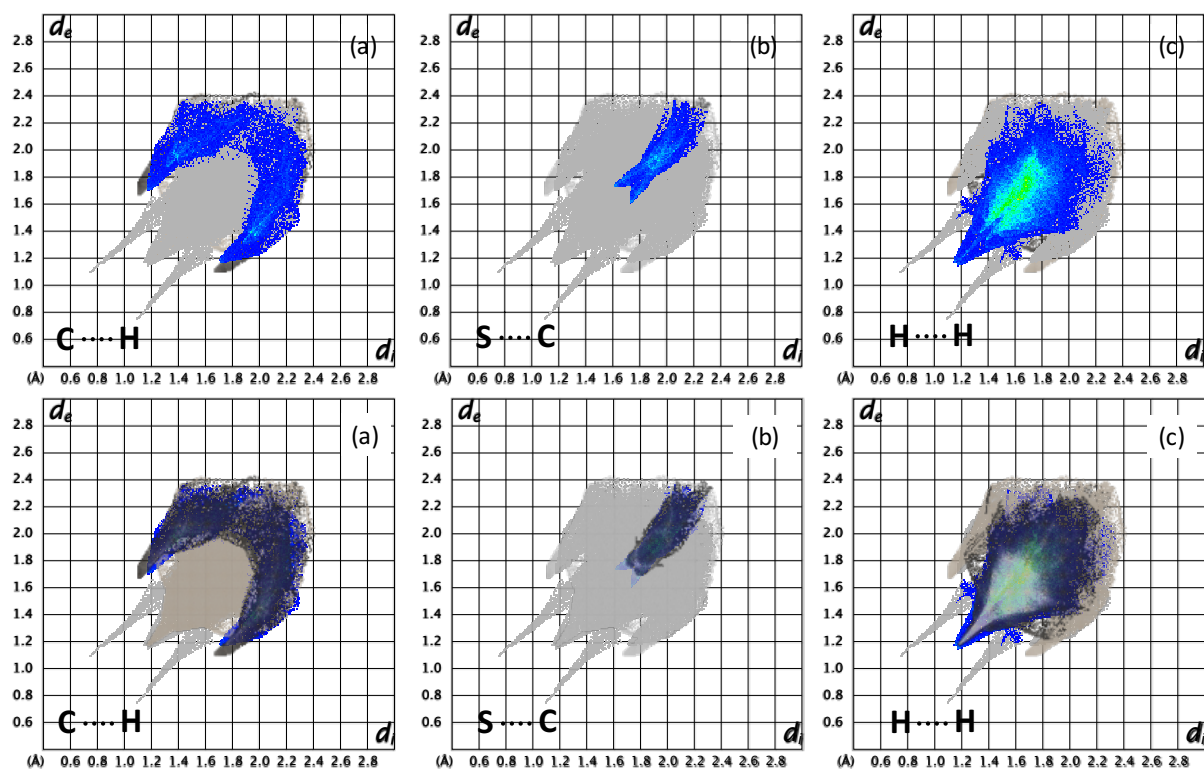


Figure S9. Superimposition of fingerprints for of C...H (a); S...C (b); H...H (c) interaction in C8-BTBT-C8 (dark) and **5** (blue). (first line C8-BTBT-C8 background, second line foreground).

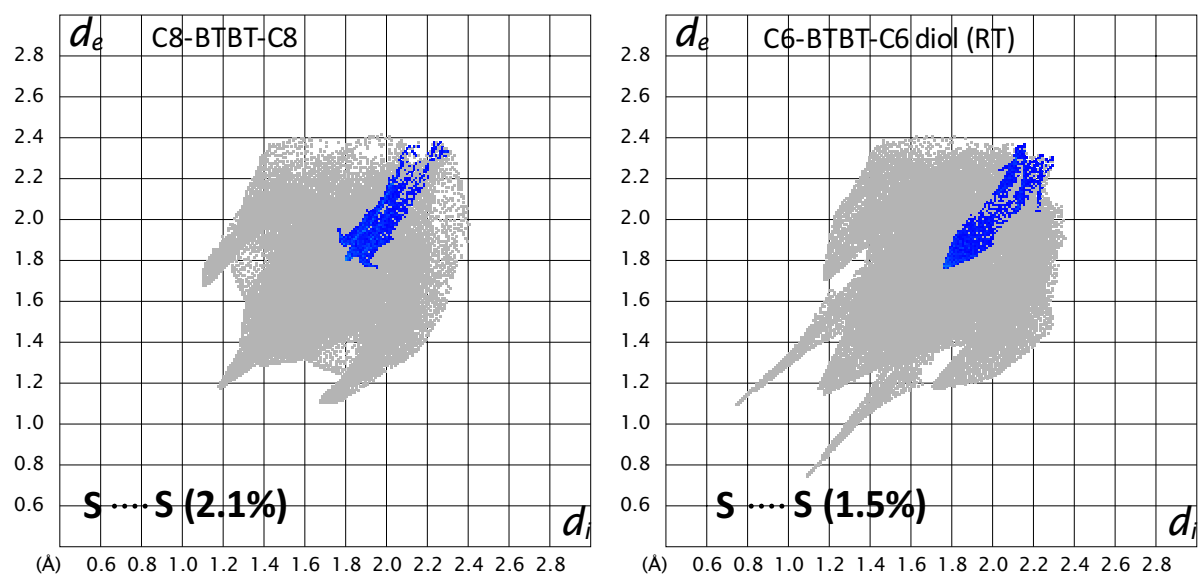


Figure S10. 2D S...S interaction fingerprints for C8-BTBT-C8 and **5**.

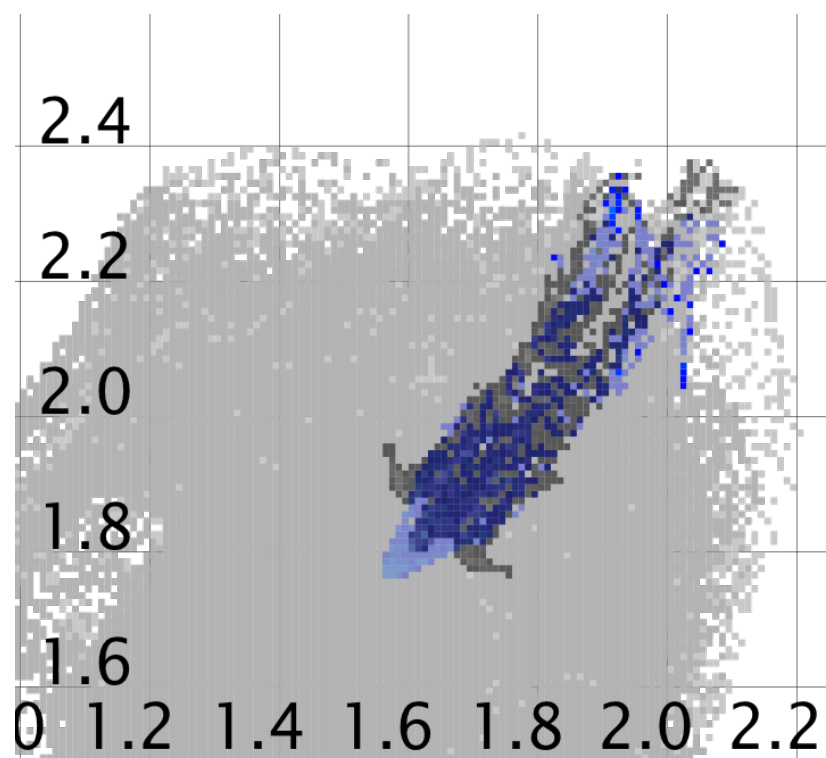


Figure S11. Superimposition of 2D S...S interactions fingerprints for C8-BTBT-C8 (dark) and **5** (blue).

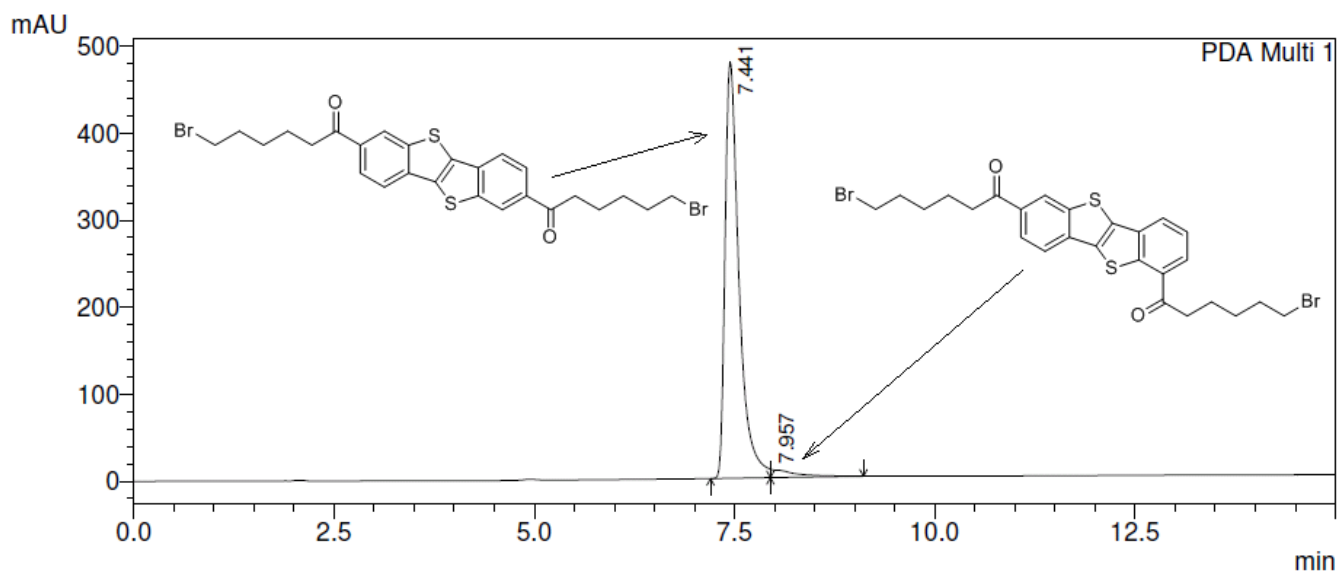


Figure S12. 2,7-diacetylated BTBT 3 HPLC chromatogram.

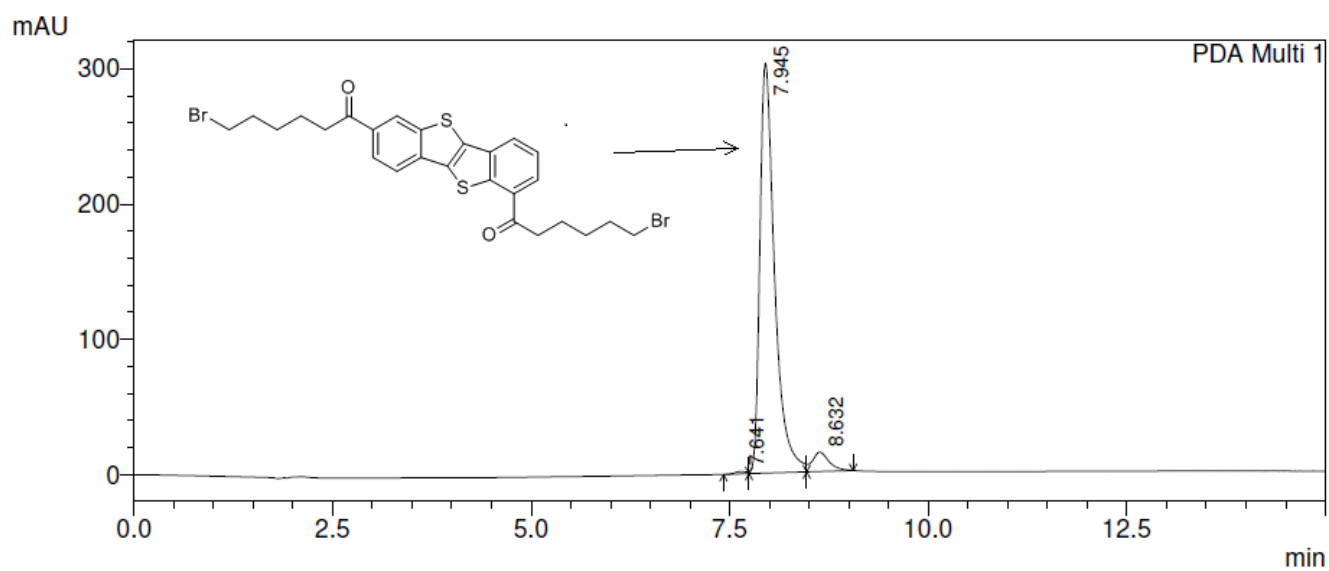


Figure S13. 1,7-diacetylated BTBT 3' HPLC chromatogram.



Figure S14. Set-up used to record the FTIR behavior of **5** as a function of the temperature. **5** was disposed in a screw sealed cell built from two slices of crystalline KBr. It was deposited by drop casting between two KBr Slices. a) KBr sealed cell; b) KBr opened cell; c) KBr sealed cell disposed in the Perkin-Elmer Spectrum 100 FT-IR spectrometer.

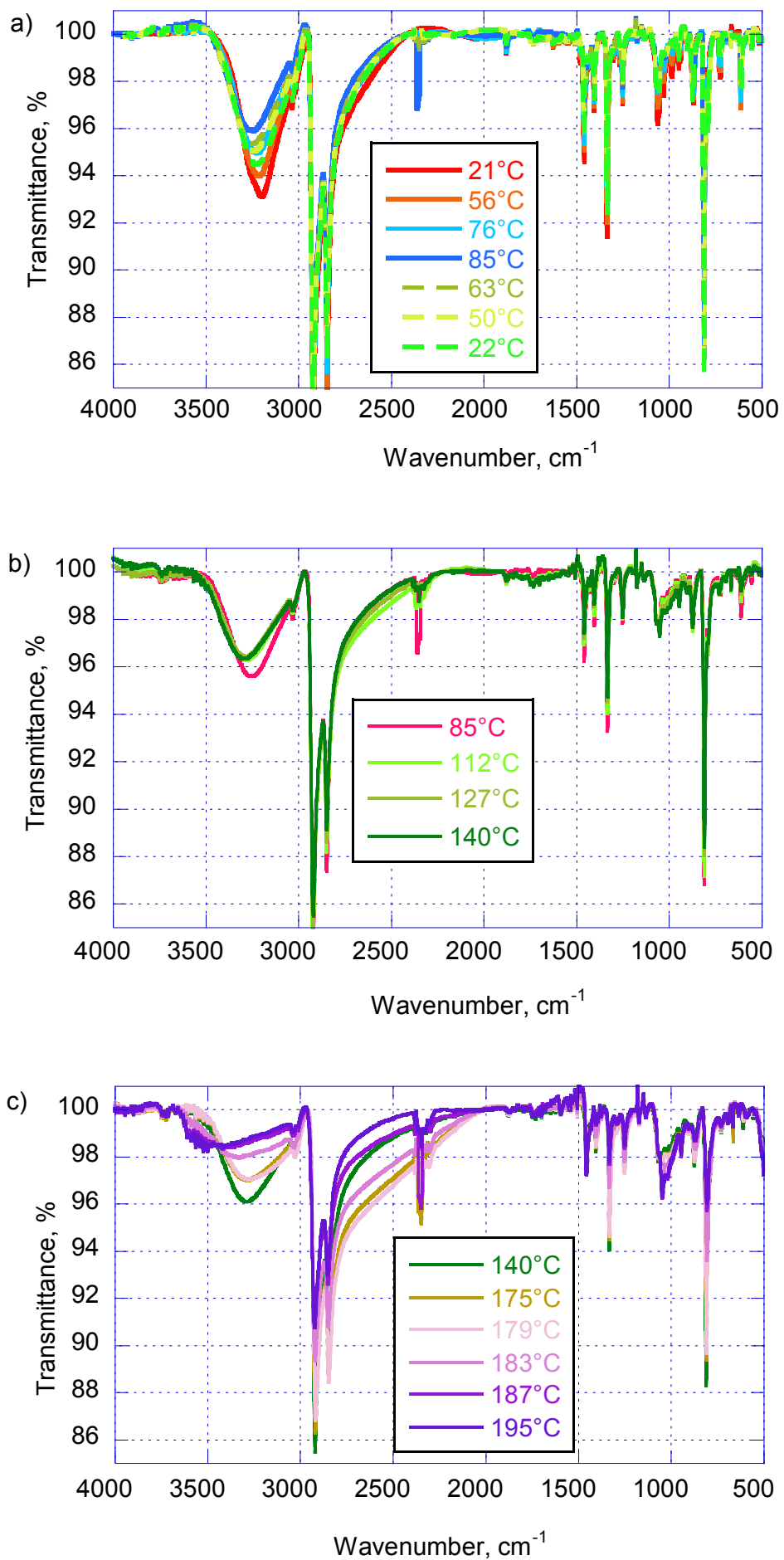


Figure S15. FT-IR full spectra of a freshly recrystallized diol **5** heated from room temperature to 195°C.

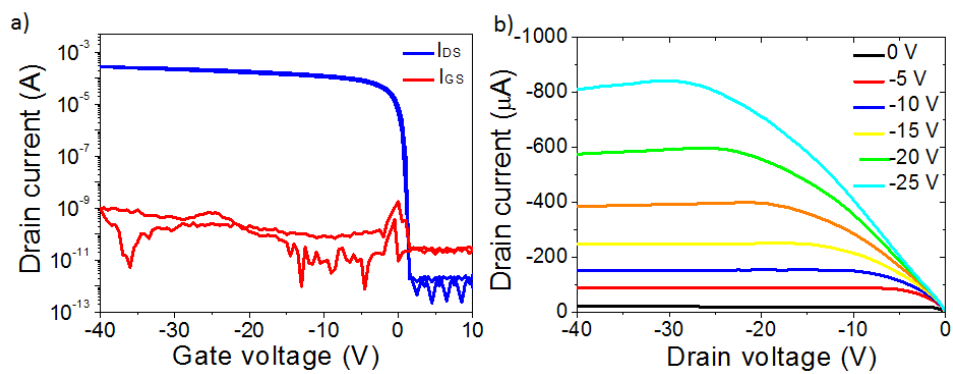


Figure S16. a) Transfer characteristics of thermally evaporated C8-BTBT-C8 based OFET in linear regime, at $V_{D_S} : -5V$, b) corresponding output characteristics for different V_{G_S} . Calculated mobilities were 1.0 and $1.8 \text{ cm}^2 \cdot \text{V}^{-1} \cdot \text{s}^{-1}$ in linear and saturation regime respectively.

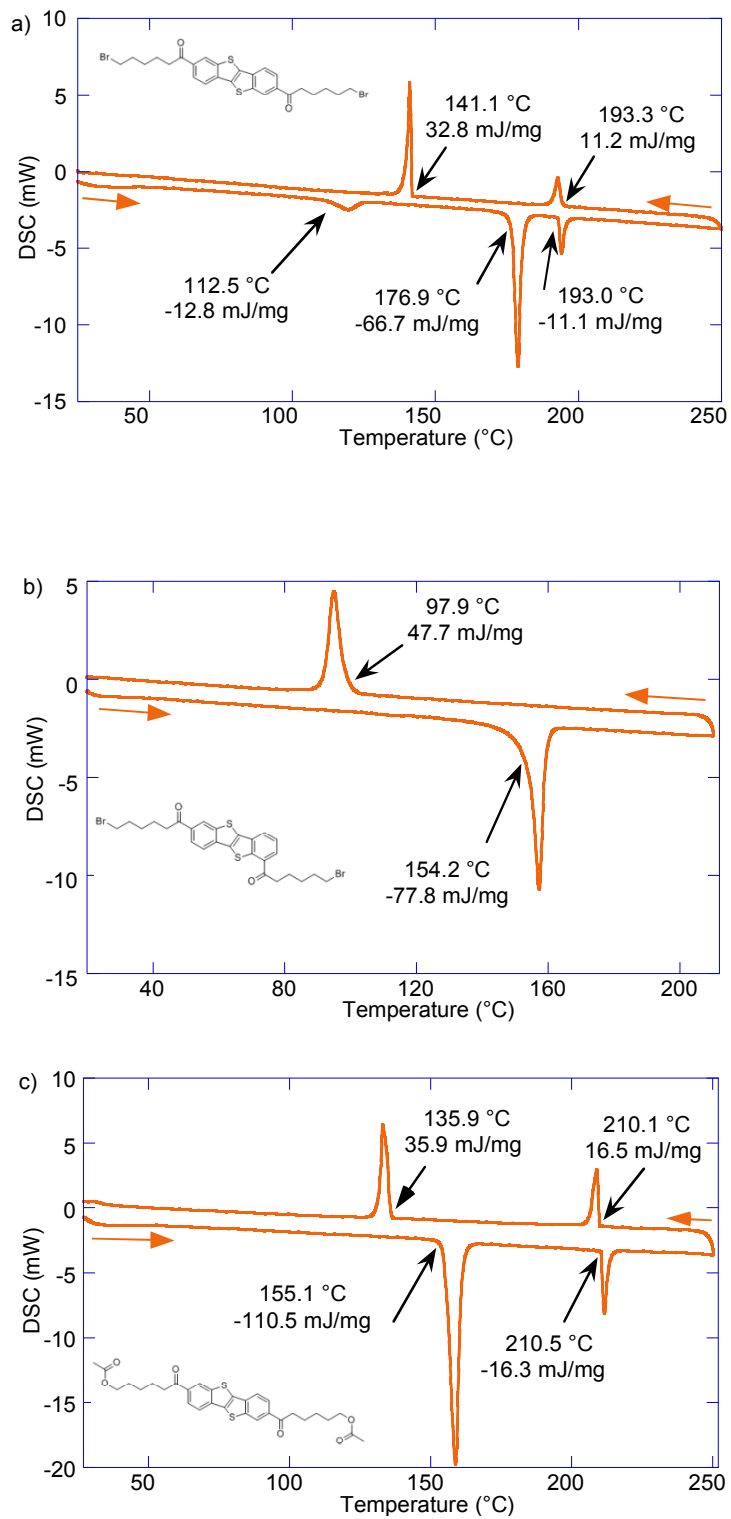


Figure S17. DSC thermograms of **3** (a), **3'** (b) and **4** (c) realized at 10°C/min

To get further information on charge injection, frontier orbitals energy levels of the diol **5** were determined from its UV-Vis spectrum and cyclic voltammogram (Figure S18). The HOMO level was estimated⁵ from the onset of oxidation peaks ($E_{\text{onset solide}} = +0.76 \text{ V}$ $E_{\text{onset liquide}} = +0.77 \text{ V}$) to be at $\approx -5.56 \text{ eV}$. The HOMO-LUMO gap estimated from the absorption edge in the UV-vis spectrum ($\lambda_{\text{edge}} = 339 \text{ nm}$) was of 3.66 eV , which gave an energy LUMO level at -1.90 eV . Those values were in good agreement with HOMO and LUMO levels of Cn-BTBT-Cn ($n = 5-14$) respectively at ca -5.5 eV and -2.0 eV .⁶

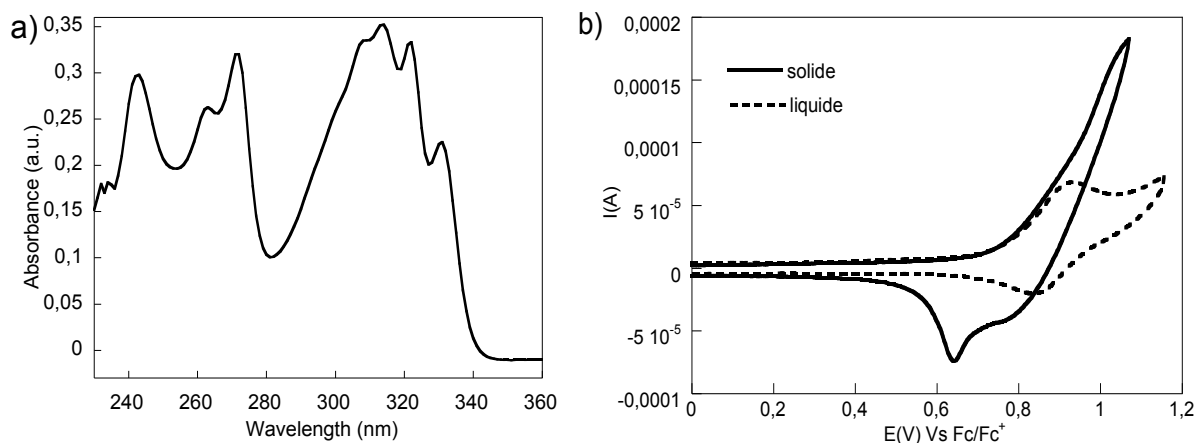


Figure S18. a) **5** UV-vis spectrum in CHCl_3 , b) Cyclic voltammogram of a 10^{-3} M solution of **5** in an electrolyte (0.1 M Bu_4NPF_6 in tetrahydrofuran solution) at room temperature with a scan rate of 100 mV/s. Ferrocene was added to calibrate the curves. Potential are given versus $E_{\text{Fc}/\text{Fc}^+}$.

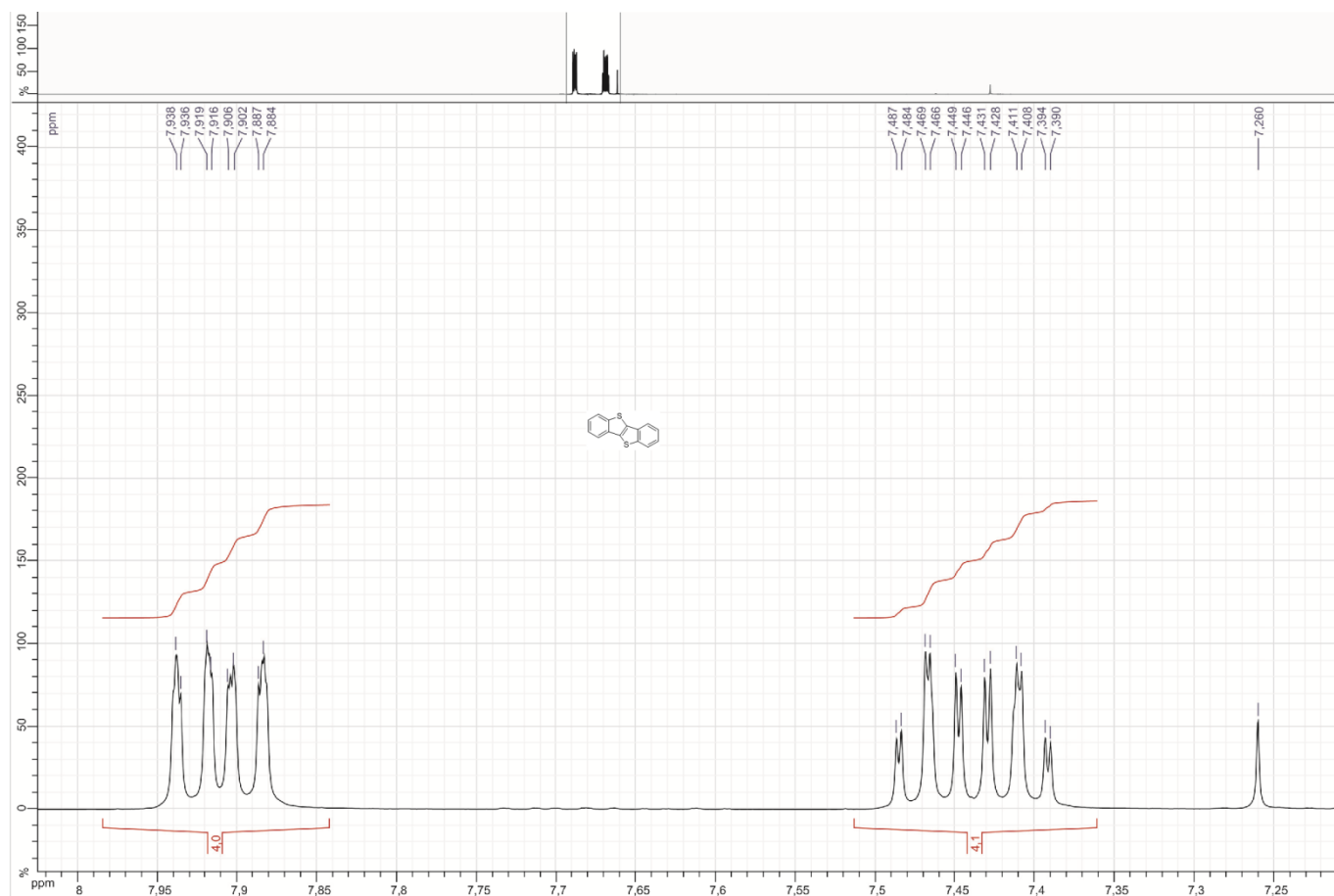


Figure S19. NMR ^1H spectrum of **2** in CDCl_3 .

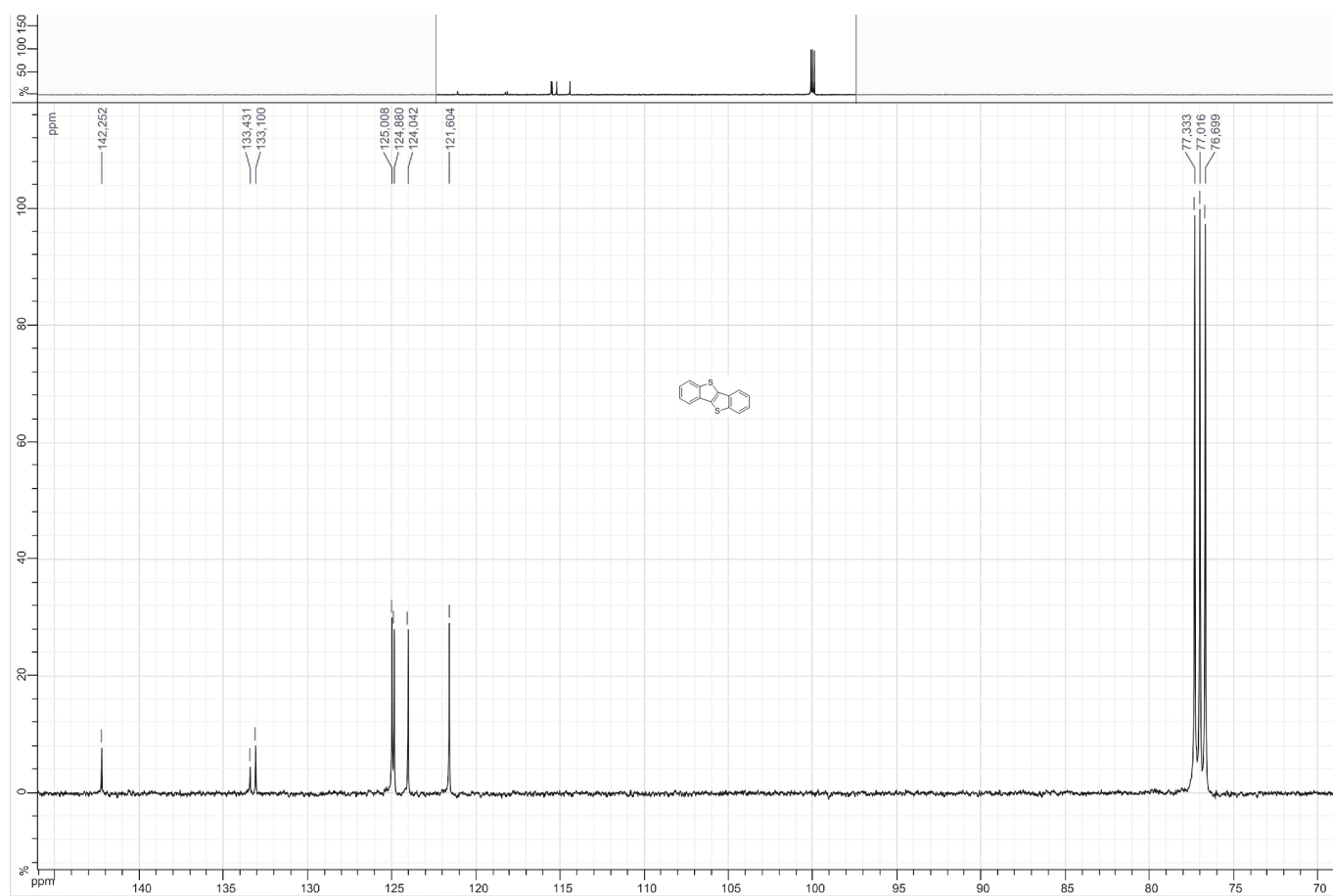


Figure S20. NMR ^{13}C spectrum of **2** in CDCl_3 .

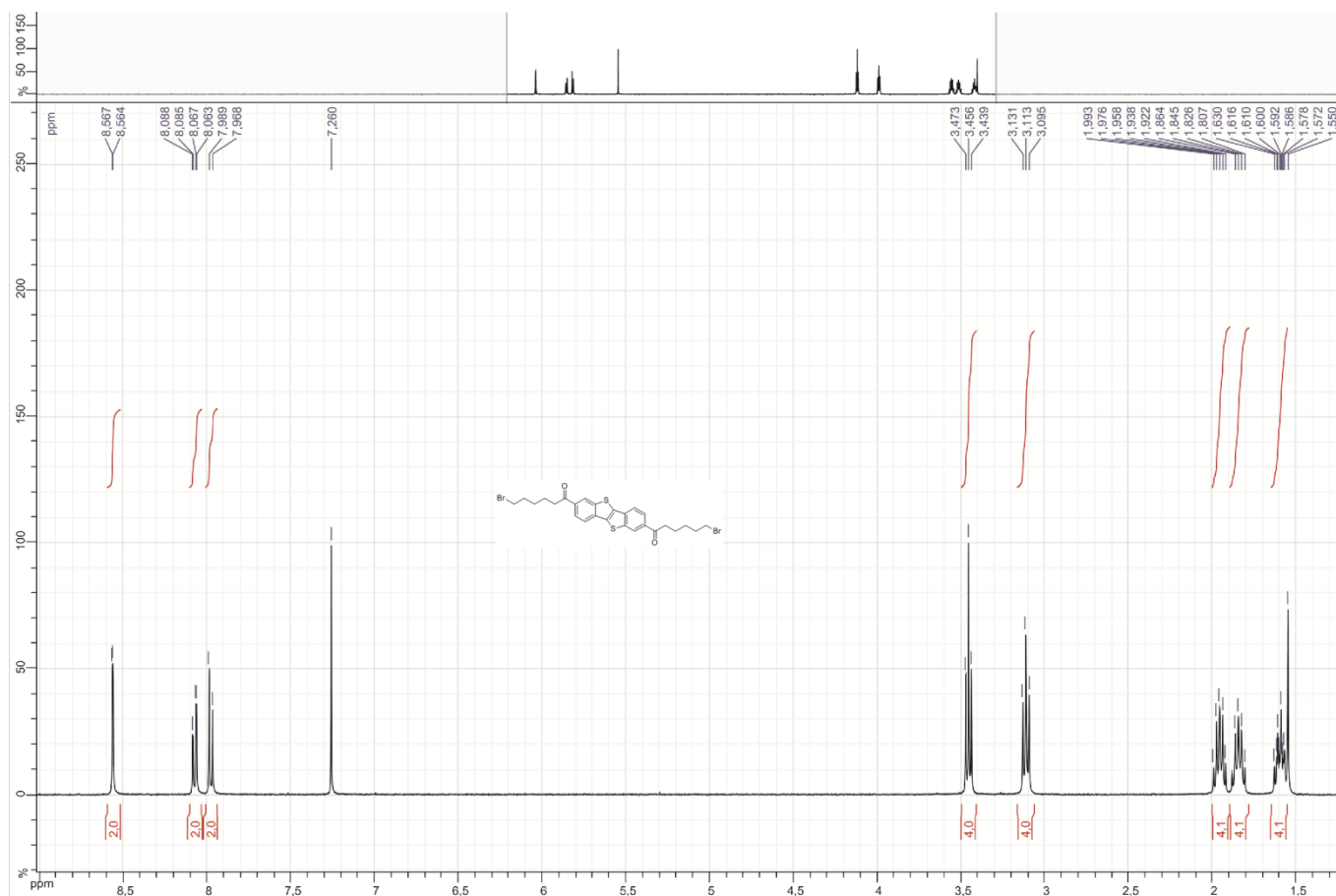


Figure S21. NMR ^1H spectrum of **3** in CDCl_3 .

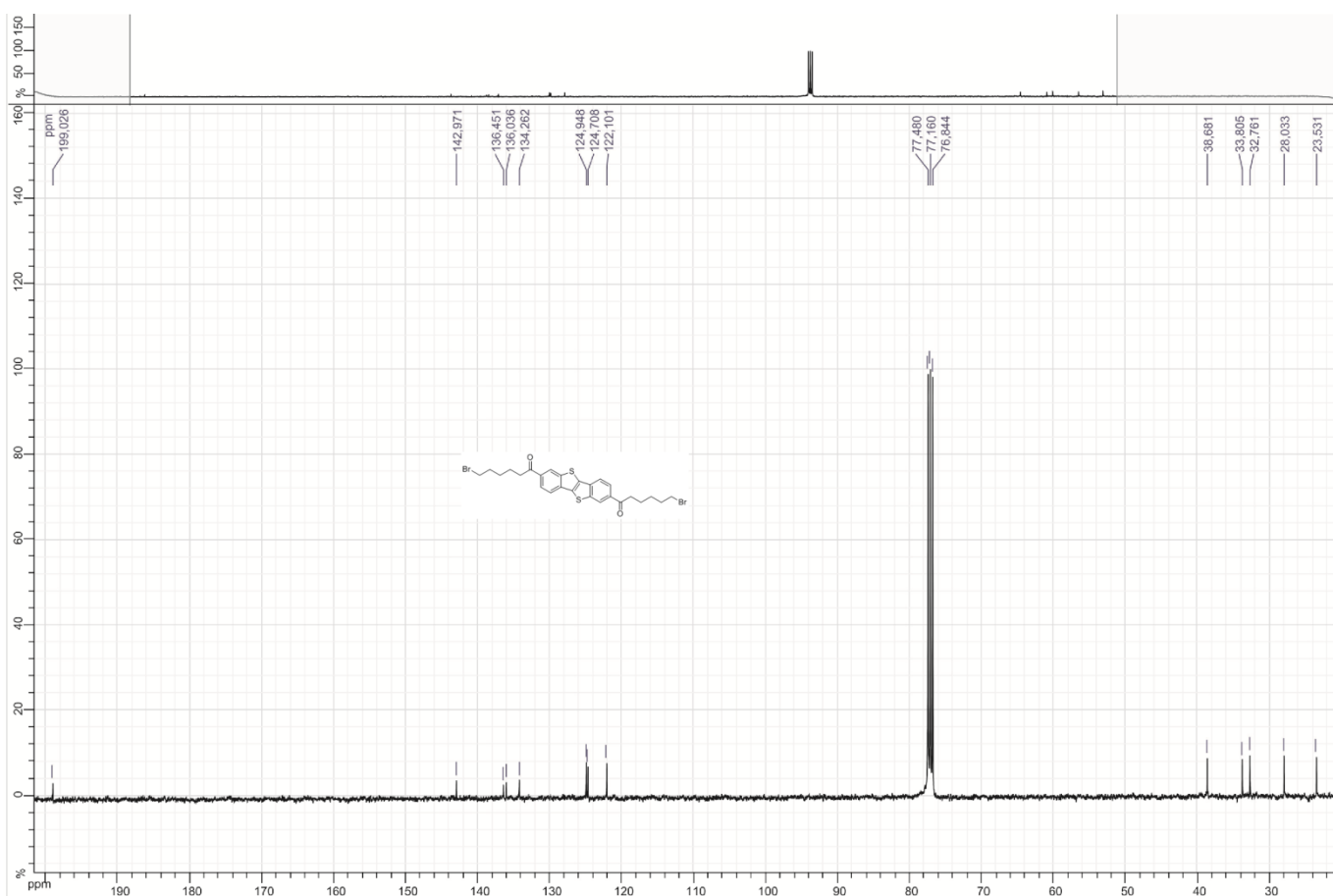


Figure S22. NMR ^{13}C spectrum of **3** in CDCl_3 .

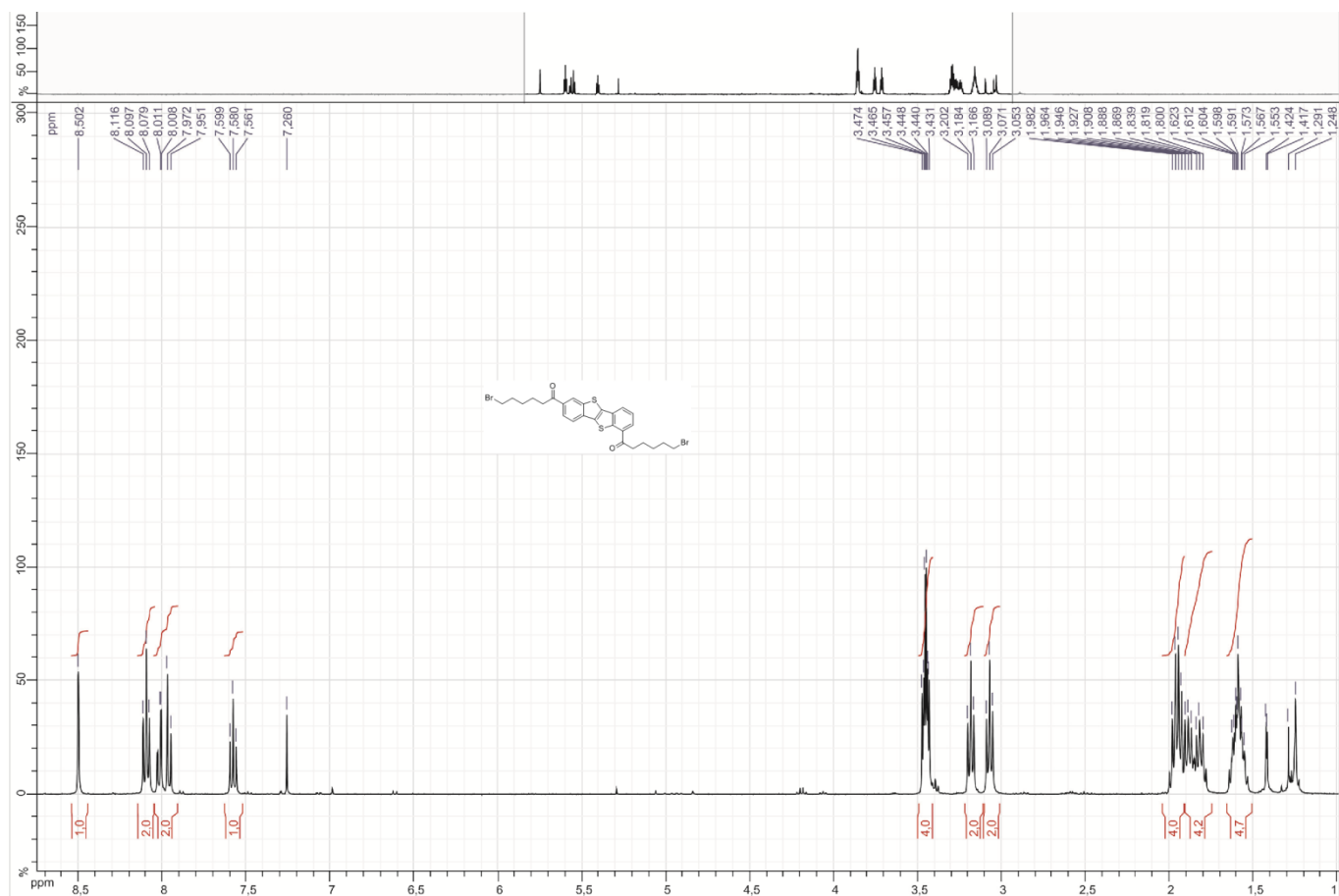


Figure S23. NMR ^1H spectrum of **3'** in CDCl_3 .

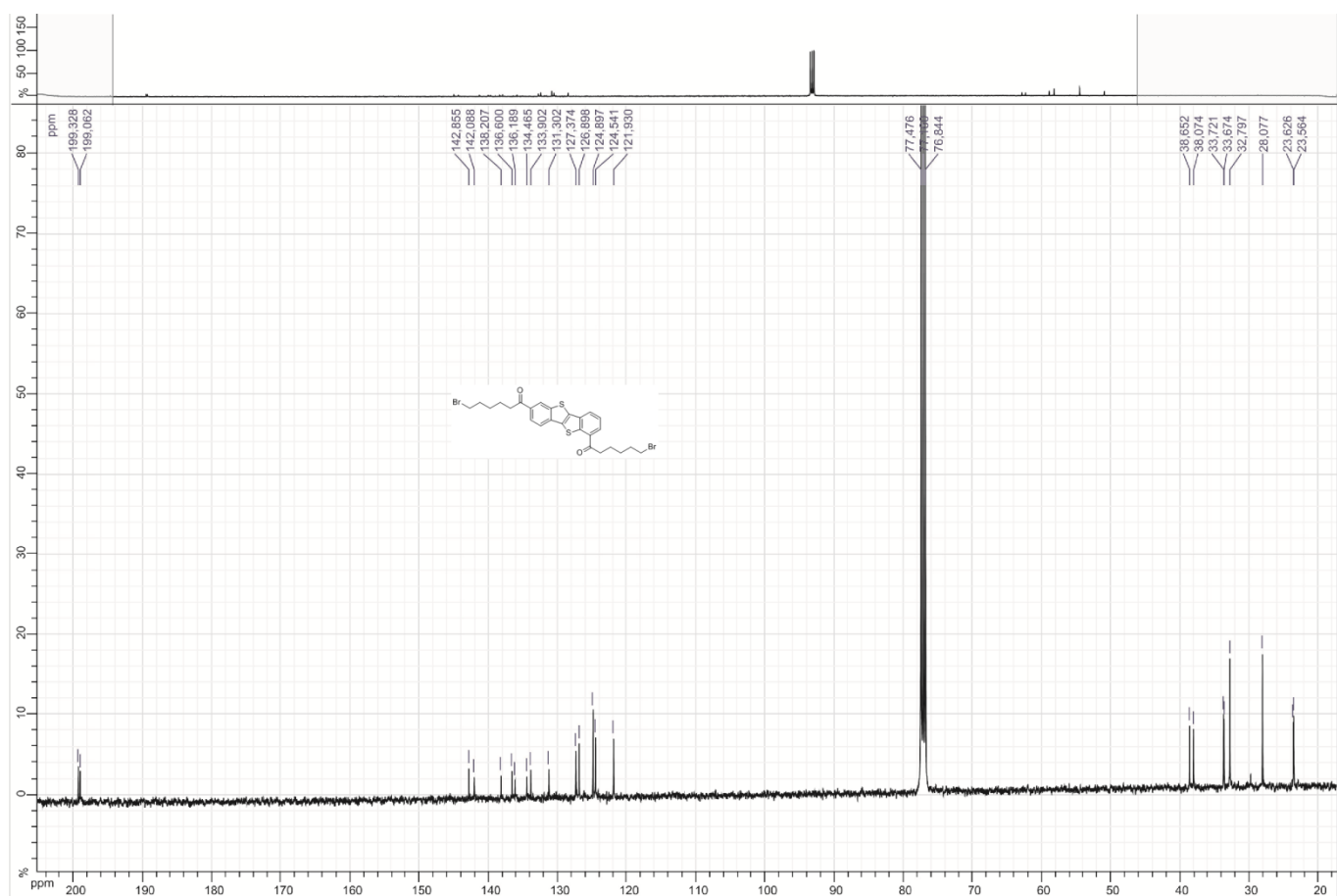


Figure S24. NMR ^{13}C spectrum of **3'** in CDCl_3 .

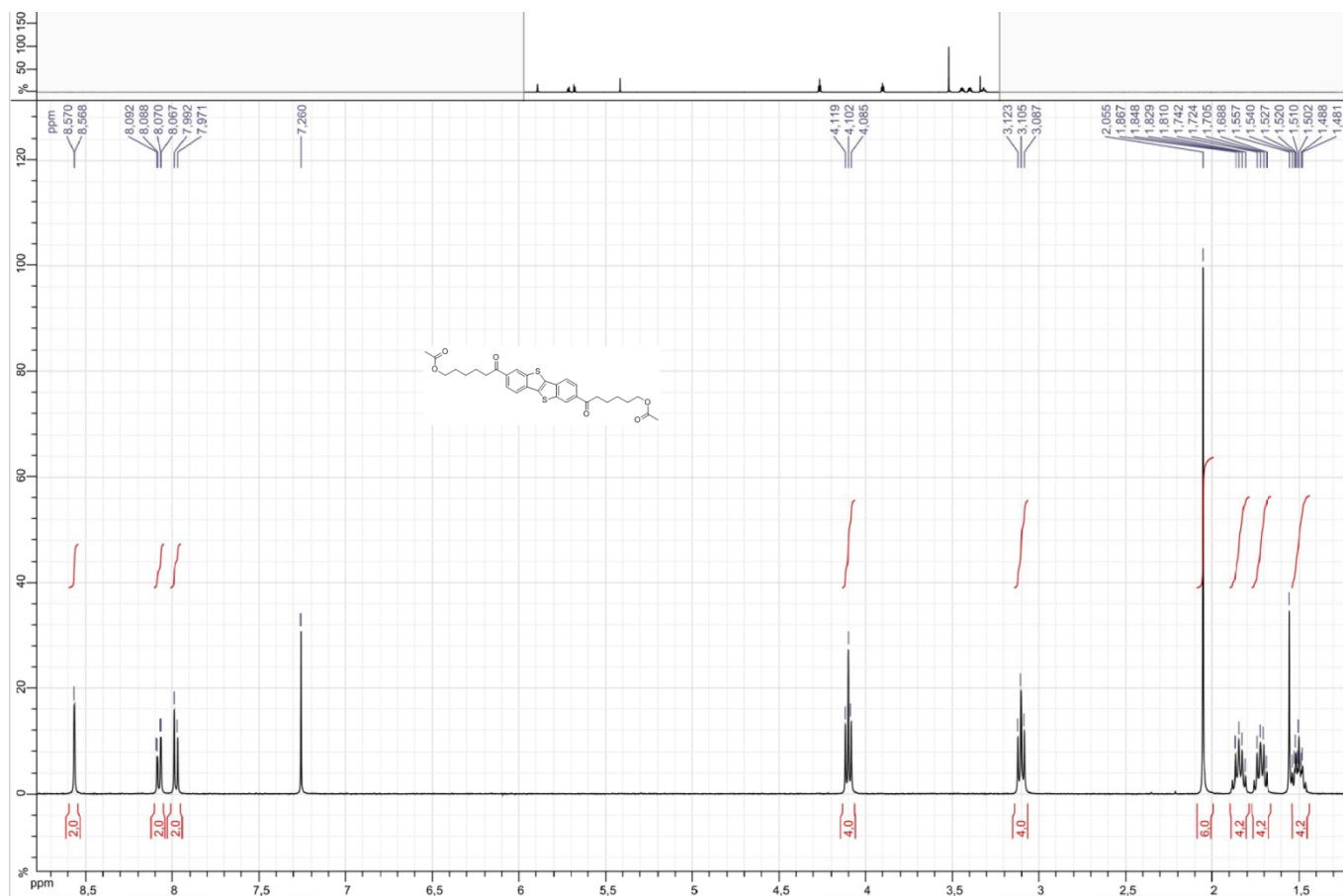


Figure S25. NMR ^1H spectrum of 4 in CDCl_3 .

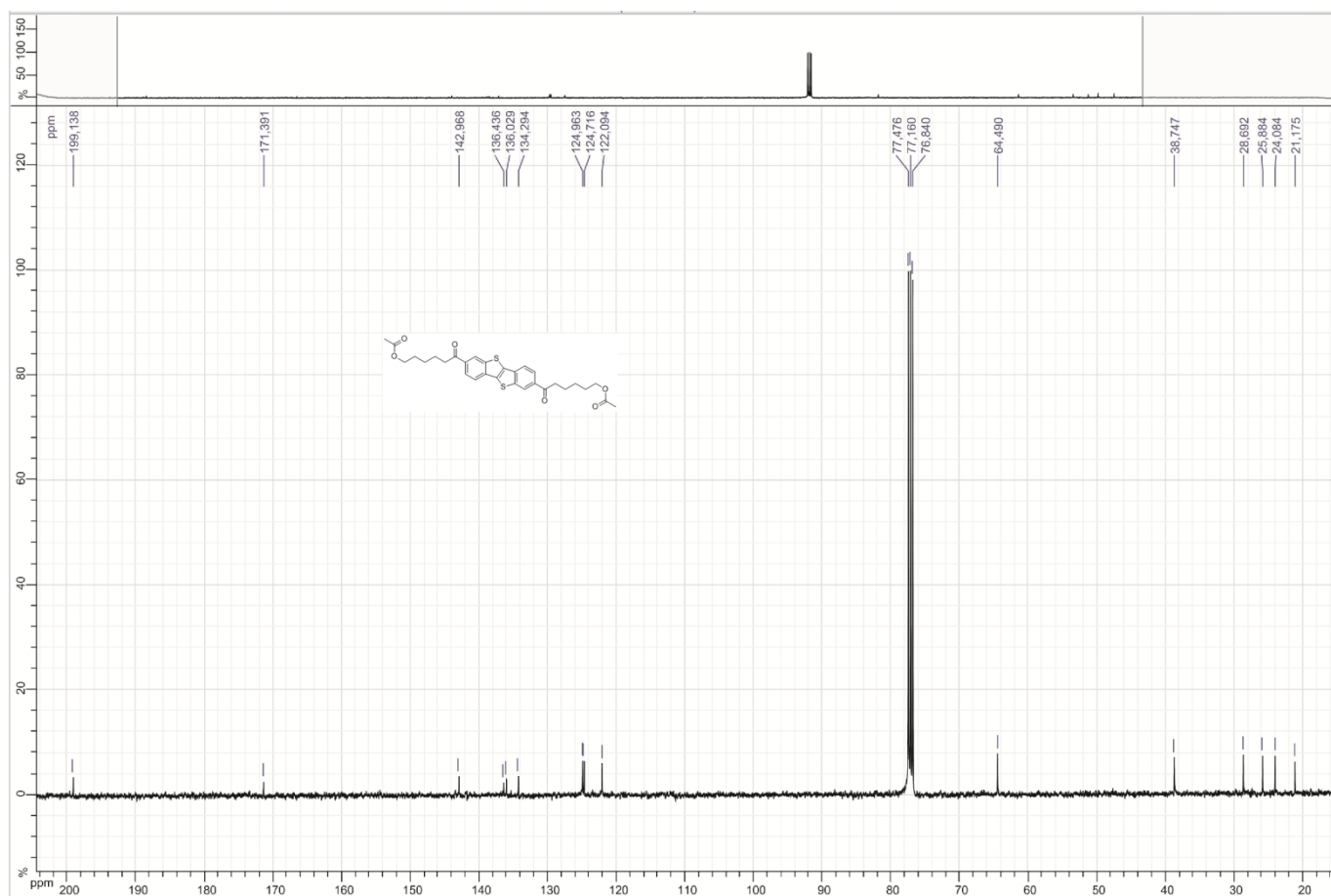


Figure S26. NMR ^{13}C spectrum of 4 in CDCl_3 .

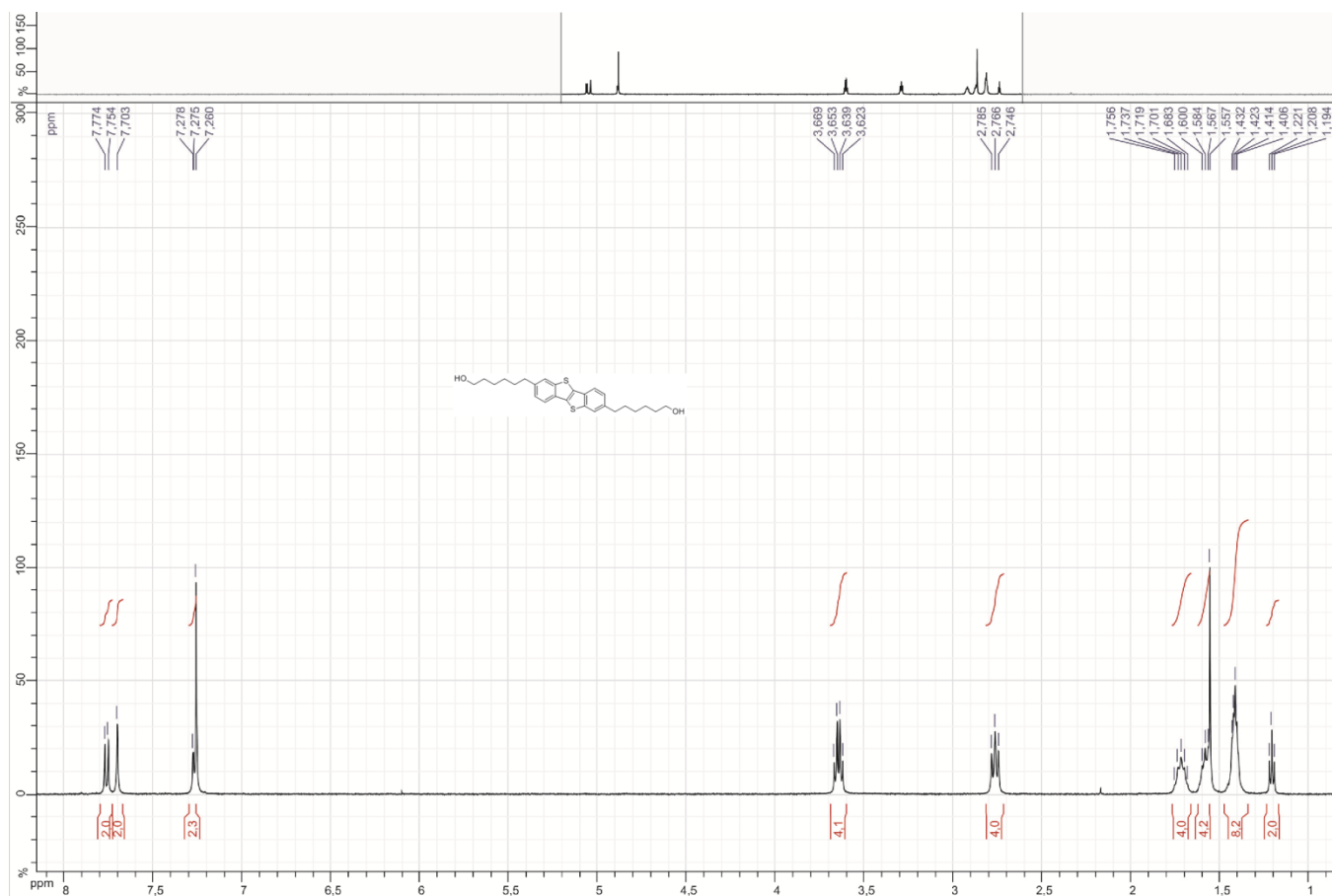


Figure S27. NMR ¹H spectrum of **5** in CDCl₃.

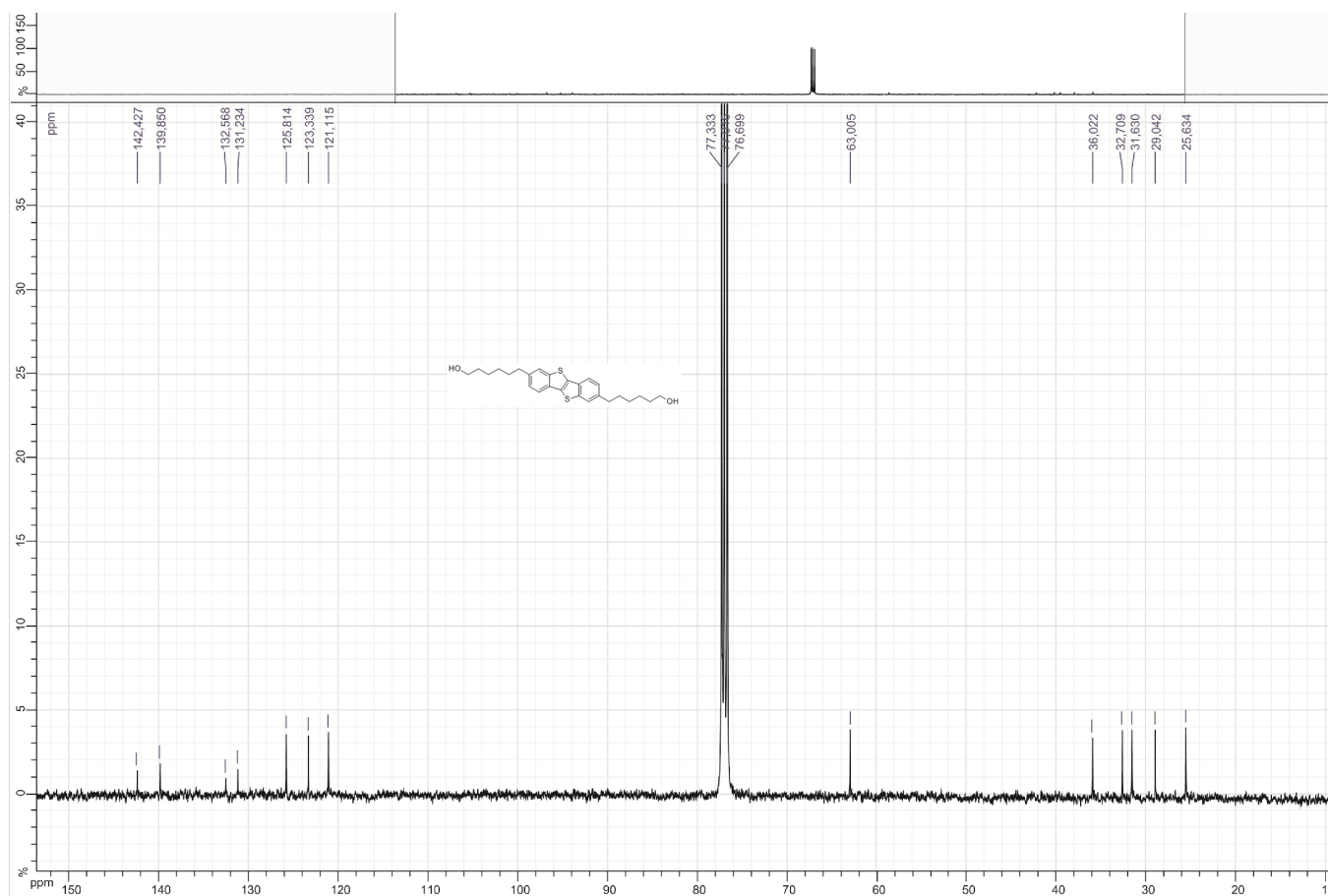


Figure S28. NMR ¹³C spectrum of **5** in CDCl₃.

-
- ¹ Hanna, J.; Hiroya K. Organic semiconductor material having molecular orientation property and showing charge injection promotor function, *JP2013041984A*, **2013**.
- ² Castet, F.; Aurel, P.; Fritsch, A.; Ducasse, L.; Liotard, D.; Linares, M.; Cornil, J.; Beljonne, D. *Phys. Rev. B* **2008**, *77*, 115210.
- ³ Hirshfeld, F. L. Bonded-atom fragments for describing molecular charge densities. *Theoretica chimica acta*, **1977**.
- ⁴ Spackman M. A.; McKinnon, J. J. Fingerprinting intermolecular interactions in molecular crystals. *CrystEngComm*. **2002**, *4*, 378–392, 2002.
- ⁵ Brédas, J.-L.; Silbey, R.; Boudreaux, D.S.; Chance, R.R. Chin-Length Dependence of Electronic and Electrochemical Properties of Conjugated Systems: Polyacetylene, Polyphenylene, Polythiophene, and Polypyrrole. *J. Am. Chem. Soc.* **1983**, *105*, 6555–6559.
- ⁶ Ebata, T. I. H.; Miyazaki, E.; Takimiya, K.; Ikeda, M.; Kuwabara, H.; Yui, T. Highly Soluble [1]Benzothieno[3,2-]benzothiophene (BTBT) Derivatives for High-Performance, Solution-Processed Organic Field-Effect Transistors. *J. Am. Chem. Soc.* **2007**, *129*, 15732-15733.